

IONIC LIQUIDS AS ADDITIVES ON THE ELECTRODEPOSITION
OF COBALT, NICKEL AND ITS ALLOY ONTO COPPER IN
ACIDIC SULFATE BATH

INAM MOHAMMEDAYOUB OMAR

UNIVERSITI TEKNOLOGI MALAYSIA

IONIC LIQUIDS AS ADDITIVES ON THE
ELECTRODEPOSITION OF COBALT, NICKEL AND ITS ALLOY
ONTO COPPER IN ACIDIC SULFATE BATH

INAM MOHAMMEDAYOUB OMAR

A thesis submitted in fulfilment of the
requirements for the award of the degree of
Doctor of Philosophy

Faculty of Science
Universiti Teknologi Malaysia

FEBRUARY 2022

ACKNOWLEDGEMENT

While conducting this thesis, I was in communication with several individuals, academics, researchers, and practitioners. They have dedicated themselves to my thoughts and understanding. In particular, I would like to express my deep and sincere appreciation for guidance, encouragement, friendship, critique, inspiration and advice to my main supervisors of my thesis, Professor Dr. Madzlan Bin Aziz and Professor Dr. Khadijah Mohammad Emran. This thesis would not be the same as presented here without their continued encouragement and involvement. I am also thankful to my co-supervisor Dr. Siti Aminah Setu for her guidance. Many thankful for Dr. Abdo Mohammed Al-Fakih and Dr. Areej Al-Garni for their guidance, teaching, advices and cooperation.

I also acknowledge the funding of my PhD research through the Join Supervision Program (JSP) to Universiti Teknologi Malaysia (UTM) and Taibah University.

Very and special thankful to Professor Dr. Khadijah Mohammad Emran, and Scientific Research Agency in Taibah University to guarantee with the budget all chemicals, materials, and devices needed to complete the experimental part of this thesis. Thankful for Professor Dr. Nadjat Rezki and Professor Dr. Mouslim Messali from chemistry department and laboratory technician Abdoulah Jaber from physic department, college of science, in Taibah University for their cooperation.

From the bottom of my heart, I would like to express my deep, boundless thanks to the soul of my beloved father, may God have mercy on him, and to my beloved mother, may God prolong her life, who put me on the path to a PhD long ago, for all the unconditional support they gave me through this research, for their wisdom. Advice and sympathetic ear. They are always there for me.

I am grateful to my husband and my child for their patient, kind, support and collaboration, and all my family members.

ABSTRACT

The electrocatalytic properties of nickel (Ni), cobalt (Co) and nickel-cobalt (Ni-Co) alloy coating qualified them to be utilized in industrial applications. Traditional organic additives have been used to enhance the deposits properties but some of them are not eco-friendly and obtained low deposits quality. Green ionic liquids (ILs) have become an alternative additive to be used in the electrodeposition due to their excellent properties. In the present study, the influence of two new ILs, namely, 1-methyl-3-((2-oxo-2-(2,4,5 trifluorophenyl) amino)ethyl)-1H-imidazol-3-ium iodide ([MOFIM]I) and 1-(4-fluorobenzyl)-3-(4- phenoxybutyl)imidazol-3-ium bromide ([FPIM]Br) were investigated as green additives for Ni, Co and Ni-Co alloy electrodeposition from acidic sulfate bath on a copper substrate. The resultant surface morphologies demonstrated that both studied ILs served as effective leveling agents but [MOFIM]I was more effective than [FPIM]Br owing to their molecular structures. Both studied ILs led to the formation finer-grained, more ordinated crystals, compact, free-cracked and highly uniform Ni, Co and Ni-Co alloy deposits compared to that obtained from free ILs bath as shown by scanning electron microscopic (SEM) studies. Atomic force microscopic (AFM) analyses exhibited that the roughness of all films deposited with [MOFIM]I were lower than that with [FPIM]Br. Both ILs led to a homogeneous distribution of the Ni and Co elements and confirmed the Ni-Co formation, as shown by the EDX-mapping. The X-ray diffraction (XRD) patterns exhibited the fcc crystal structures with (2 2 0) was preferred growth orientation of the Ni, Co and Ni-Co alloys crystallites without and with both studied ILs. The average crystallite size of the Ni, Co and Ni-Co alloy films decreased by 30%, 12% and 27% respectively with [MOFIM]I and by 25%, 5% and 18% respectively with [FPIM]Br. The microhardness of the Ni, Co and Ni-Co alloys increased in the presence of both ILs. All voltametric measurements indicated that the inhibition of Co^{2+} and Ni^{2+} reduction in the presence of both ILs occurred *via* their adsorption on the cathode surface, which obeyed the Langmuir adsorption isotherm. The optimal bath conditions that led to the highest CCE% values involved a current of 20 mA cm^{-2} , deposit potential of 6.5 V, pH of 4.5, temperature of 25°C and deposit time of 10 min. The percentage current efficiency (CCE%) values of Ni, Co and Ni-Co alloy electrodeposition were very high (nearly 100%) in the presence of both studied ILs. The highest corrosion resistance was for Ni deposit in the NaCl solution with [MOFIM]I, compared to that with [FPIM]Br. However, Co deposit exhibited lowest corrosion resistance with [MOFIM]I and [FPIM]Br respectively. Ni-Co₂ and Ni-Co₃ alloys deposited at the optimal conditions were the two best alloys to resist corrosion among all the Ni-Co alloys examined in the current study. The co-deposition of Ni-Co alloy obeyed the anomalous type. This anomalous behavior was alleviated after [MOFIM]I and [FPIM]Br were introduced in the Ni-Co deposition baths. Quantum chemical calculations were performed at the B3LYP/6-311++G(d,p) level of the density functional theory (DFT). Several quantum parameters and natural atomic charges were calculated. The results showed that the calculated values of the quantum parameters and natural atomic charges were consistent with the experimental findings.

ABSTRAK

Sifat elektromangkin nikel (Ni), kobalt (Co) dan aloi nikel-kobalt melayakkan mereka digunakan dalam aplikasi industri. Bahan aditif organik tradisional telah digunakan untuk menambahbaik sifat enapan tetapi sebahagiannya tidak berkualiti dan tidak mesra persekitaran. Cecair ionik (IL) hijau telah menjadi alternatif untuk digunakan dalam menghasilkan elektroenapan yang sangat baik. Dalam kajian ini kesan dua cecair ionik, iaitu, 1-metil-3-((2-okso-2-(2,4,5-trifluorofenil)amino)etil)-1H-imidazol-3-ium iodida ([MOFIM]I) and 1-(4-fluorobenzil)-3-(4-fenoksibutil)imidazol-3-ium bromida ([FPIM]Br) dikaji sebagai bahan tambahan hijau untuk elektroenapan Ni, Co dan aloi Ni-Co di atas substrat kuprum daripada media sulfat. Hasil morfologi permukaan menunjukkan kedua IL berperanan sebagai agen pelaras tetapi [MOFIM]I adalah lebih berkesan daripada [FPIM]Br disebabkan oleh struktur molekulnya. Kedua IL menyebabkan pembentukan butiran halus berkrystal yang tersusun, padat, bebas retak dan endapan Ni, Co dan Ni-Co yang seragam seperti ditunjukkan oleh kajian mikroskopi imbasan elektron (SEM). Analisis mikroskopi daya atom (AFM) menunjukkan penurunan kekasaran permukaan yang diendap oleh [MOFIM]I berbanding [FPIM]Br. Kedua IL menyebabkan penyerakan Ni, Co yang lebih seragam selain pembentukan aloi Ni-Co yang ditunjukkan oleh pemetaan EDX. Corak pembiasan sinar-X (XRD) menunjukkan Ni, Co dan Ni-Co terendap berstruktur hablur fcc dengan (2 2 0) sebagai orientasi tumbuh terpilih samada dengan kehadiran IL atau tidak. Purata saiz hablur dalam filem Ni, Co dan aloi Ni-Co berkurangan masing-masing sebanyak 30%, 12% dan 27% dengan [MOFIM]I dan masing-masing 25%, 5% dan 18% dengan [FPIM]Br. Kekerasan mikro Ni, Co dan aloi Ni-Co juga bertambah dengan kehadiran kedua IL. Semua pengukuran voltametrik menunjukkan bahawa penghalangan penurunan Co^{2+} and Ni^{2+} dengan kehadiran IL berlaku melalui penjerapan di atas permukaan katod yang mematuhi isoterma penjerapan Langmuir. Keadaan mandian optimum yang memberikan %CCE tertinggi melibatkan arus 20 mA cm^{-2} , keupayaan endapan 6.5 V, pH 4.5, suhu 25°C dan masa endapan selama 10 min. Nilai %CCE elektroendapan Ni, Co dan aloi Ni-Co adalah sangat tinggi (hampir 100%) dengan kehadiran kedua IL yang dikaji. Rintangan kakisan tertinggi adalah untuk endapan Ni di dalam larutan NaCl dengan [MOFIM]I berbanding [FPIM]Br. Walau bagaimanapun, endapan Co menunjukkan rintangan kakisan terendah di dalam [MOFIM]I dan [FPIM]Br. Aloi Ni-Co₂ and Ni-Co₃ yang dimendapkan pada keadaan optimum adalah dua aloi terbaik untuk menghalang kakisan di kalangan semua aloi Ni-Co yang diselidiki dalam kajian ini. Ko-enapan aloi Ni-Co mematuhi jenis anomali. Sifat anomali ini ditingkatkan setelah [MOFIM]I dan [FPIM]Br digunakan di dalam mandian endapan Ni-Co. Pengiraan Kuantum Kimia dilakukan pada aras teori fungsi ketumpatan (DFT) B3LYP/6-311++G (d, p). Beberapa parameter kuantum dan cas atom tabii telah dikira. Keputusan menunjukkan nilai pengiraan parameter kuantum dan cas atom tabii adalah konsisten dengan dapatan eksperimen.

TABLE OF CONTENTS

	TITLE	PAGE
	DECLARATION	iii
	DEDICATION	iv
	ACKNOWLEDGEMENT	v
	ABSTRACT	vi
	ABSTRAK	vii
	TABLE OF CONTENTS	viii
	LIST OF TABLES	xvii
	LIST OF FIGURES	xviii
	LIST OF ABBREVIATIONS	xxv
	LIST OF SYMBOLS	xxvi
	LIST OF APPENDICES	xxvii
CHAPTER 1	INTRODUCTION	1
	1.1 Background of Study	1
	1.2 Properties, Corrosion Resistance and Structure of Nickel, Cobalt and Ni-Co Alloy Electrodeposits	2
	1.3 Mechanism of Ni, Co and Ni-Co alloy electrodeposition	4
	1.4 Applications of Nickel, Cobalt and Ni-Co Alloys in Industry	5
	1.4.1 Applications of Nickel	5
	1.4.2 Applications of Cobalt	6
	1.4.3 Applications of Ni-Co alloy	6
	1.5 Additives in the Electrodeposition Process	7
	1.5.1 Organic and Inorganic Additives.	7
	1.5.2 Mechanism of Additives	8
	1.6 Ionic Liquids (ILs)	9
	1.6.1 Ionic Liquid as Additives	11

1.7	Quantum Chemical Calculation	11
1.8	Problem Statement	12
1.9	Research Objectives	15
1.10	Scope of the Research	16
1.11	Significant of the Study	18
1.12	Outline of the Thesis	18
CHAPTER 2	LITERATURE REVIEW	20
2.1	Introduction	20
2.2	Nickel Electrodeposition	21
2.3	Cobalt Electrodeposition	23
2.4	Ni-Co Alloy Electrodeposition	25
2.5	Additives in the Electrodeposition Process	27
2.5.1	Effect of Additives on the Nucleation Mechanism	32
2.6	Ionic Liquid (IL)	36
2.6.1	Structure of Ionic Liquid	36
2.6.2	Ionic Liquids Properties and Advantages	38
2.6.3	Synthesis of Ionic liquid	39
2.6.4	Applications of Ionic Liquids in the Electrodeposition	40
2.6.5	Ionic liquid as Additive or Electrolyte in the Electrodeposition	41
2.7	Mechanism of Ni, Co and Ni-Co Alloy Electrodeposition	45
2.8	Interaction between Metal Ion and Ionic Liquid	49
2.9	Adsorption Isotherm Models	52
2.9.1	Langmuir Isotherm Model	53
2.9.2	Temkin Isotherm Model	53
2.9.3	Flory–Huggins Isotherm Model	54
2.10	Quantum Chemical Calculations	55
2.10.1	Background	55

	2.10.2 Quantum Chemical Calculations on Additives in the Electrodeposition and Corrosion Inhibitors in the Corrosion Inhibition Processes	55
	2.10.3 Limitations of Computational Methods	58
	2.11 Chapter Summary	59
CHAPTER 3	RESEARCH METHODOLOGY	73
3.1	Introduction	73
3.2	Ionic Liquid Preparation	73
3.3	Composition of the Electrodeposition Baths	75
3.4	Electrodes	78
3.5	Electrodes Preparation	79
3.6	Cells Design and Operation	80
	3.6.1 Cell Design	80
	3.6.2 Electrochemical Setup	80
3.7	Experimental Procedure	82
	3.7.1 Electrodeposition and Cathodic Current Efficiency (CCE%)	82
	3.7.2 Voltammetric Measurements	84
	3.7.2.1 Potentiodynamic Cathodic Polarization (CP)	84
	3.7.2.2 Cyclic Voltammetry (CV)	85
	3.7.2.3 In-Situ Anodic Linear Stripping Voltammetry (ALSV)	85
	3.7.3 Adsorption Isotherm	86
	3.7.4 Deposit Characterizations	87
	3.7.4.1 Scanning Electron Microscopy (SEM) and Energy Dispersive X-Ray Spectrometry (EDX)	87
	3.7.4.2 X-Ray Diffraction (XRD)	87
	3.7.4.3 Atomic Force Microscopy (AFM)	88

	3.7.5	Microhardness Measurements	88
	3.7.6	Electrochemical Corrosion Behavior	88
	3.8	Theoretical Calculations Methodology	89
	3.9	Chapter Summary	90
CHAPTER 4		RESULTS AND DISCUSSION OF COBALT AND NICKEL ELECTRODEPOSITION IN PRESENCE OF [MOFIM]I AND [FPIM]Br IONIC LIQUIDS	91
	4.1	Introduction	91
	4.2	Outline of this Chapter	91
	4.3	Section A: Electrodeposition of Cobalt and Nickel with [MOFIM]I Ionic Liquid	92
	4.3.1	Cathodic Polarization (CP)	92
	4.3.2	Tafel Lines and Electrode Kinetics	96
	4.3.3	Adsorption Isotherm	98
	4.3.3.1	Langmuir Adsorption Isotherm	99
	4.3.3.2	Temkin and Flory–Huggins Adsorption Isotherm	100
	4.3.3.3	Effect of Iodide Ions on the Electrodeposition	101
	4.3.4	Cyclic Voltammetry	102
	4.3.5	Anodic Linear Stripping Voltammetry (ALSV)	105
	4.3.6	Cathodic Current Efficiency	106
	4.3.7	Crystal Structure and Surface Morphology	109
	4.3.8	Electrochemical Impedance Spectroscopy (EIS)	120
	4.3.9	Potentiodynamic Polarization	122
	4.4	Section B: Electrodeposition of Cobalt and Nickel with [FPIM]Br Ionic Liquid	123
	4.4.1	Cathodic Polarization (CP)	123
	4.4.2	Tafel Lines and Electrode Kinetics	127
			128

4.4.3	Adsorption Isotherms	128
4.4.3.1	Langmuir Adsorption Isotherm	
4.4.3.2	Temkin and Flory–Huggins Adsorption Isotherm	130
4.4.3.3	Effect of Bromide Ions on the Electrodeposition	130
4.4.4	Cyclic Voltammetry	131
4.4.5	Anodic Linear Stripping Voltammetry (ALSV)	133
4.4.6	Cathodic Current Efficiency	135
4.4.7	Crystal Structure and Surface Morphology	136
4.4.8	Electrochemical Impedance Spectroscopy (EIS)	146
4.4.9	Potentiodynamic Polarization	148
4.5	Chapter Summary	148
CHAPTER 5	RESULTS AND DISCUSSION OF NICKEL- COBALT ALLOY ELECTRODEPOSITION IN PRESENCE OF [MOFIM]I AND [FPIM]Br IONIC LIQUIDS	150
5.1	Introduction	150
5.2	Outline of this Chapter	151
5.3	Section A: Compositions, CCE%, Characterization and Microhardness of Ni-Co Alloy Coating	151
5.3.1	Composition of Ni-Co Alloy	151
5.3.2	Cathodic Current Efficiency (CCE%)	154
5.3.3	Physical Characterizations	156
5.3.4	Phase Composition	165
5.3.5	Surface Topography and Roughness	168
5.3.6	Microhardness	173
5.3.7	Nucleation and Growth Mechanism of Ni, Co and Ni-Co alloy deposits	174

5.4	Section B: Corrosion Resistance and Voltametric Behavior of Ni-Co Alloy Deposited from Ni70-Co30% Bath.	
5.4.1	Electrochemical Impedance Spectroscopy (EIS)	176
5.4.2	Potentiodynamic Polarization	176
5.4.3	Comparison Among Ni, Co and Ni-Co Alloy Electrodeposition	179
5.4.4	Potentiodynamic Cathodic Polarization	182
5.4.5	Tafel Lines and Electrode Kinetics	184
5.4.6	Adsorption Isotherms	187
5.4.6.1	Langmuir Adsorption Isotherm	188
5.4.6.2	Temkin and Flory–Huggins Adsorption Isotherm	189
5.4.7	Cyclic Voltammetry	190
5.4.8	Anodic Linear Stripping Voltammetry (ALSV)	191
5.5	Interaction between Co and/or Ni Ions and Ionic Liquid Ions	193
5.5.1	Effect of [MOFIM]I and [FPIM]Br Ionic Liquid Cations on the Co, Ni and Ni-Co Alloy Electrodeposition	195
5.5.2	Effect of [MOFIM]I and [FPIM]Br Ionic Liquid Anions on the Co, Ni and Ni-Co Alloy Electrodeposition	196
5.6	Chapter Summary	197
		199
CHAPTER 6	QUANTUM CHEMICAL CALCULATIONS	201
6.1	Introduction	201
6.2	Outline of this Chapter	202
		202

6.3	The Active Centers in the [MOFIM]I and [FPIM]Br	207
6.4	Section A: Quantum Chemical Parameters	211
6.5	Section B: Natural Atomic Charge (Mulliken charges)	215
6.6	The Mechanism of Ni, Co and Ni-Co Alloy Electrodepositions in the Presence of [MOFIM]I and [FPIM]Br	218
6.7	Structure and Properties of [MOFIM]I and [FPIM]Br	224
6.8	Chapter Summary	
CHAPTER 7	CONCLUSION AND RECOMMENDATIONS	225
7.1	Conclusions	225
7.1.1	Ni and Co Electrodeposition in Presence of [MOFIM]I and [FPIM]Br ILs as Additive	225
7.1.2	Ni-Co alloy Electrodeposition in Presence of both [MOFIM]I and [FPIM]Br ILs	228
7.1.3	Quantum Chemical Calculations	229
7.1.4	Reasons of Higher Enhancement Effect of [MOFIM]I Compared to [FPIM]Br	230
7.2	Scope of Further Study	233
	REFERENCES	234
	APPENDICES	249

LIST OF TABLES

TABLE NO.	TITLE	PAGE
Table 2.1	Summary of the previous studies of Ni, Co and Ni-Co alloy electrodeposition.	59
Table 2.2	Summary of the additives function in mechanism of electrodeposition reported in the previous studies.	56
Table 3.1	The bath composition for Ni and Co electrodeposition, the operating conditions and the electrodes using for Ni, Co and Ni-Co alloy electrodeposition.	77
Table 3.2	The composition of Ni-Co alloys baths in absence and presence of [MOFIM]I and [FPIM]Br.	78
Table 4.1	CPP of Co and Ni electrodeposition at 2.0×10^{-3} mA.cm ⁻² in the absence and presence of different [MOFIM]I concentrations and θ by [MOFIM]I at different concentrations.	94
Table 4.2	Tafel kinetic parameters obtained for Co and Ni deposits in the absence and presence of different concentrations of [MOFIM]I.	98
Table 4.3	NOP and the height of anodic current (i_a) peaks of ALSVs for Co and Ni electrodeposition in the absence and presence of different concentrations of [MOFIM]I.	103
Table 4.4	The operating conditions of Co and Ni electrodepositions which used at CCE% studies.	107
Table 4.5	CCE%, Co and Ni deposits appearance under optimal bath conditions in the absence and presence of different concentrations of [MOFIM]I.	108

Table 4.6	The grain size, R_a and R_t of Co and Ni deposits obtained from SEM, XRD and AFM analysis in the absence and presence of [MOFIM]I and [FPIM]Br.	118
Table 4.7	Fitting the results from EIS and polarization measurements in 3.5% NaCl and average microhardness of Co and Ni deposits without and with 1×10^{-5} M [MOFIM]I at 25°C.	122
Table 4.8	CPP of Co and Ni electrodepositions at 2.0×10^{-3} mAcm ⁻² without and with different concentrations of [FPIM]Br and θ by different concentrations of at ~ -1.3 V _{SCE} .	126
Table 4.9	Tafel kinetic parameters obtained for Co and Ni different plating solutions.	128
Table 4.10	NOP and the height of anodic peaks of ALSV measurements for Co and Ni electrodeposition in the absence and presence of different concentrations of [FPIM]Br.	132
Table 4.11	Co and Ni deposits appearance and color under optimal bath conditions in the absence and presence of different concentrations of [FPIM]Br.	136
Table 4.12	Fitting results from EIS and polarization measurements for Co and Ni deposits in 3.5% NaCl in the absence and presence [FPIM]Br.	147
Table 5.1	C.R.L., Ni and Co contents in Ni-Co alloys and CCE% in the absence and presence of [MOFIM]I and [FPIM]Br at the optimum conditions.	153
Table 5.2	Comparison of the obtained results of Ni-Co ₂ and Ni-Co ₃ alloys coating in the presence of 1×10^{-5} M [MOFIM]I and [FPIM]Br with other best bath composition in the presence of additives.	156
Table 5.3	The grain size, R_a and R_t of Ni-Co alloy deposits obtained from SEM, XRD and AFM analysis in the absence and presence of [MOFIM]I and [FPIM]Br.	165

Table 5.4	Fitting the results from EIS and polarization measurements for the nine Ni-Co alloys deposits in 3.5% NaCl.	178
Table 5.5	Tafel slope, b_c and kinetic parameters of Ni, Co and Ni-Co1 alloy electrodeposition from acidic baths.	184
Table 5.6	Cathodic polarization potential (CPP) of Ni-Co alloy electrodepositions from bath1 at 5.0×10^{-3} mA.cm ⁻² without and with different concentrations of [MOFIM]I and [FPIM]Br and surface coverage (θ) by both ILs at different concentrations.	186
Table 5.7	Tafel slope and kinetic parameters obtained for Ni-Co alloy electrodepositions from bath1 without and with different concentrations of [MOFIM]I and [FPIM]Br.	188
Table 5.8	Langmuir Isotherm results of [MOFIM]I and [FPIM]Br adsorption on Ni-Co alloy deposited from bath1	190
Table 5.9	NOP of CV measurements and the height of anodic peaks, i_a , of ALSV measurements for Ni-Co alloy electrodeposition from bath1 without and with different concentrations of [MOFIM]I and [FPIM]Br.	192
Table 6.1	The differences between the molecular structures of two ionic liquid imidazole additives during electrodeposition to Ni, Co and Ni-Co alloy.	202
Table 6.2	Quantum chemical parameters of Neutral and cation species of [MOFIM]I and [FPIM]Br calculated at the B3LYP/6-311++G(d,p) level of DFT. IE_{Rct} (%) of Ni-Co2 and Ni-Co3 alloys.	208
Table 6.3	The natural atomic charges of each atom in neutral and cation forms of [MOFIM]I molecule.	213
Table 6.4	The natural atomic charges of each atom in neutral and cation forms of [FPIM]Br molecule.	214

LIST OF FIGURES

FIGURE NO.	TITLE	PAGE
Figure 1.1	Schematic steps illustrated the mechanism of the formation Ni, Co and Ni-Co alloy electrodeposits.	5
Figure 1.2	Examples of different Ni, Co and Ni-Co alloy coatings applied on components in various industries.	7
Figure 2.2	Schematic illustration of the molecular structure of cations from the ionic liquids.	37
Figure 2.3	Synthesis of a) imidazolium-based	40
Figure 2.4	Mechanism of hydrogen evolution reaction	47
Figure 2.5	Schematic diagram of mechanism of Ni, Co and/or Ni-Co alloy electrodeposition in presence of IL additive.	49
Figure 2.6	The octahedrally coordinated nickel or cobalt complexes in the aqueous system	50
Figure 1.3	The molecular structure of the ionic liquids (a) [MOFIM]I, (b) [FPIM]Br.	16
Figure 2.1	The diagram of nucleation process: (a) instantaneous and (b) progressive.	33
Figure 3.1	The electroplating cell and the electrochemical setup for (a) the electrodeposition and CCE%, (b) potentiodynamic CP and corrosion resistance, (c) CV and ALSV.	82

Figure 4.1	Potentiodynamic cathodic polarization (CP) curves for (a) Co and (b) Ni electrodeposition in the absence and presence of different concentrations of [MOFIM]I at pH 4.5.	94
Figure 4.2	Langmuir adsorption isotherm for [MOFIM]I adsorption on Cu substrate during (a) Co, (b) Ni electrodeposition.	99
Figure 4.3	CVs for (a) Co and (b) Ni electrodepositions recorded at GCE in the absence and presence of different concentrations of [MOFIM]I at scan rate 100 mV/sec.	102
Figure 4.4	CVs for (a) Co and (b) Ni electrodeposition at 1×10^{-5} M [MOFIM]I recorded at GCE with different scan rates. Inset linear relation between cathodic peak current density (i_{cp}) as a function of the scan potential rate $v^{1/2}$ in the R-S plot.	104
Figure 4.5	ALSVs and i_a peaks for (a, c) Co and (b, d) Ni electrodeposition on GCE in the absence and presence of different [MOFIM]I concentrations.	106
Figure 4.6	SEM images, high magnification SEM and EDX spectra of (a, a', a'') Cu substrate, (b, b', b'') Co deposited from free [MOFIM]I, (c, c', c'') Co deposited with 1×10^{-5} M [MOFIM]I, (d, d', d'') Co deposited with 1×10^{-3} M [MOFIM]I.	112
Figure 4.7	SEM images, high magnification SEM and EDX spectra of Ni deposited from bath (a, a', a'') free [MOFIM]I, (b, b', b'') 1×10^{-4} M [MOFIM]I, (c, c', c'') 5×10^{-6} M [MOFIM]I, (d, d', d'') 1×10^{-5} M [MOFIM]I.	114
Figure 4.8	AFM 3D, 2D images, of (a, a') pure copper (substrate), Co deposited from bath (b, b') free-[MOFIM]I, (c, c') 1×10^{-5} M [MOFIM]I, (d, d') 1×10^{-3} M [MOFIM]I.	116

Figure 4.9	AFM 3D, 2D images, of Ni deposited from bath (a, a') free-[MOFIM]I, (b, b') 1×10^{-4} M [MOFIM]I, (c, c') 5×10^{-6} M [MOFIM]I, (d, d') 1×10^{-5} M [MOFIM]I.	117
Figure 4.10	XRD patterns of Cu substrate, (a, a', a'') Co deposits, (b, b', b'') Ni deposits in the absence and presence of 1×10^{-5} M [MOFIM]I.	119
Figure 4.11	Nyquist plots for Cu substrate (a) Co and (b) Ni deposits in 3.5% NaCl in the absence and presence of 1×10^{-5} M [MOFIM]I. Equivalent circuit compatible with the experimental impedance data (c) Co, (d) Ni deposits.	121
Figure 4.12	Potentiodynamic polarization curves for (a) Co and (b) Ni deposits in the absence and presence of 1×10^{-5} M [MOFIM]I in 3.5% NaCl.	123
Figure 4.13	Potentiodynamic cathodic polarization (CP) curves (a) Co; (b) Ni electrodeposition in the absence and presence of different concentrations of [FPIM]Br at pH 4.5.	124
Figure 4.14	Langmuir adsorption isotherm for [FPIM]Br adsorption on Cu substrate during (a) Co, (b) Ni electrodeposition.	129
Figure 4.15	CVs for (a) Co; (b) Ni for electrodepositions at GCE in the absence and presence of different concentrations of [FPIM]Br at scan rate 100 mV/sec.	132
Figure 4.16	CVs for (a) Co; (b) Ni electrodeposition at 1×10^{-5} M [FPIM]Br recorded at GCE with different scan rates. Insert linear relation between i_{cp} as a function of the scan potential rate $v^{1/2}$.	133
Figure 4.17	ALSVs and i_a peaks for (a, c) Co; (b, d) Ni electrodepositions on GCE in absence and	135

	presence of different concentrations of [FPIM]Br.	
Figure 4.18	SEM images, high magnification SEM and EDX spectra of (a, a', a'') Cu substrate, (b, b', b'') Co deposits in free [FPIM]Br, (c, c', c'') Co deposits at 1×10^{-5} M [FPIM]Br, (d, d', d'') Co deposits at 1×10^{-4} M [FPIM]Br.	140
Figure 4.19	SEM images, high magnification SEM and EDX spectra of Ni deposits (a, a', a'') in free [FPIM]Br, (b, b', b'') 1×10^{-5} M [FPIM]Br, (c, c', c'') 1×10^{-4} M [FPIM]Br.	141
Figure 4.20	AFM 3D, 2D images, of Co deposits in the presence of (a, a') 0 M, (b, b') 1×10^{-5} M, (c, c') 1×10^{-4} M.	143
Figure 4.21	AFM 3D, 2D images, of Ni deposits in the presence of [FPIM]Br (a, a') 0 M, (b, b') 1×10^{-5} M, (c, c') 1×10^{-4} M.	144
Figure 4.22	XRD patterns of (a, a', a'') Cu substrate, Co deposits, (b, b', b'') Ni deposits in the absence and presence of 1×10^{-5} M [FPIM]Br.	145
Figure 4.23	Nyquist plots for Cu substrate (a) Co and (b) Ni in 3.5% NaCl in the absence and presence of 1×10^{-5} M [FPIM]Br. Equivalent circuit compatible with the experimental impedance data (c) Co, (d) Ni deposits.	147
Figure 4.24	Potentiodynamic polarization curves for (a) Co and (b) Ni deposited in the absence and presence of 1×10^{-5} M [FPIM]Br in 3.5% NaCl.	148
Figure 5.1	The relationship between $[Co^{2+}] / [Ni^{2+}]$ ratios in the baths and Co content in (a) C.R.L., (b) Ni-Co1, Ni-Co4 and Ni-Co7 alloys (free IL), (c) Ni-Co2, Ni-Co5 and Ni-Co8 alloys (with 1×10^{-5} M [MOFIM]I), (d) Ni-Co3, Ni-Co6 and Ni-Co9	153

	alloys (with 1×10^{-5} M [FPIM]Br), $i = 20 \text{ mA cm}^{-2}$, $t = 10 \text{ min.}$, $T = 20^\circ\text{C}$.	
Figure 5.2	Effect of $[\text{Co}^{2+}] / [\text{Ni}^{2+}]$ ratios in the bath on CCE% of (a) Ni-Co1, Ni-Co4 and Ni-Co7 alloys (free IL), (b) Ni-Co2, Ni-Co5 and Ni-Co8 alloys (with 1×10^{-5} M [MOFIM]I), (c) Ni-Co3, Ni-Co6 and Ni-Co9 alloys (with 1×10^{-5} M [FPIM]Br), $i = 20 \text{ mA cm}^{-2}$, $t = 10 \text{ min.}$, $T = 25^\circ\text{C}$.	155
Figure 5.3	SEM images, high magnification SEM of (a, a') Ni-Co1 alloy (free IL), (b, b') Ni-Co2 alloy (with 1×10^{-5} M [MOFIM]I), (c, c') Ni-Co3 alloy (with 1×10^{-5} M [FPIM]Br).	159
Figure 5.4	SEM images, high magnification SEM of (a, a') Ni-Co4 alloy (free IL), (b, b') Ni-Co5, alloy (with 1×10^{-5} M [MOFIM]I), (c, c') Ni-Co6 alloy (with 1×10^{-5} M [FPIM]Br).	160
Figure 5.5	SEM images, high magnification SEM of (a, a') Ni-Co7 alloy (free IL), (b, b') Ni-Co8, alloy (with 1×10^{-5} M [MOFIM]I), (c, c') Ni-Co9 alloy (with 1×10^{-5} M [FPIM]Br).	161
Figure 5.6	EDX spectra and SEM-EDX elemental mapping images of Cu, Co, Ni, and C, N, O, F elements of [MOFIM]I and [FPIM]Br compositions obtained from the Ni-Co alloys electrodeposited in (a),(b),(c) free ILs, (a'),(b'),(c') 1×10^{-5} M [MOFIM]I, (a''),(b''),(c'') 1×10^{-5} M [FPIM]Br.	164
Figure 5.7	XRD patterns of (a) Ni-Co1, Ni-Co2, Ni-Co3 alloys, (b) Ni-Co7, Ni-Co8, Ni-Co9 alloys, (c) Ni-Co4, Ni-Co5, Ni-Co6 alloys without and with 1×10^{-5} M [MOFIM]I and [FPIM]Br.	167
Figure 5.8	AFM 3D, 2D images, of (a, a') Cu substrate, Ni-Co alloy deposits in (b, b') Ni-Co1 alloy, (c, c') Ni-Co2 alloy, (d, d') Ni-Co3 alloy, (e, e') Ni-Co1	171

	alloy+ 5×10^{-7} M [MOFIM]I, (f, f') Ni-Co1 alloy+ 5×10^{-7} M [FPIM]Br.	
Figure 5.9	AFM 3D, 2D images, of (a, a') Ni-Co4 alloy (b, b') Ni-Co5 alloy (c, c') Ni-Co6 alloy.	172
Figure 5.10	AFM 3D, 2D images, of (a, a') Ni-Co7 alloy (b, b') Ni-Co8 alloy (c, c') Ni-Co9 alloys.	173
Figure 5.11	Nyquist plots for Cu substrate, Ni-Co alloys in 3.5% NaCl without and with 1×10^{-5} M (a) [MOFIM]I, (b) [FPIM]Br, (c) Equivalent circuit compatible with the experimental impedance data of Ni-Co alloy deposits.	178
Figure 5.12	Potentiodynamic polarization curves for (a) Cu substrate, Ni-Co1, Ni-Co2, Ni-Co3 alloys, (b) Ni-Co4, Ni-Co5, Ni-Co6 alloys, (c) Ni-Co7, Ni-Co8, Ni-Co9 alloys in 3.5% NaCl.	181
Figure 5.13	Comparison among Ni, Co and Ni-Co alloy electrodeposition by voltametric measurements (a) Potentiodynamic cathodic polarization curves, (b) CV, (c) ALSV.	183
Figure 5.14	Potentiodynamic cathodic polarization curves Ni-Co alloy electrodeposition from Ni70%-Co30% bath1 in the absence (blank) and presence of different concentrations of (a) [MOFIM]I, (b) [FPIM]Br at pH 4.5.	187
Figure 5.15	Langmuir adsorption isotherm of (a) [MOFIM]I, (b) [FPIM]Br in Ni-Co alloy electrodeposition from Ni70%-Co30% bath1.	190
Figure 5.16	CVs for Ni-Co alloy electrodeposition from Ni70%-Co30% bath1 at GCE in the absence and presence of different concentrations of (a) [MOFIM]I; (b) [FPIM]Br from acidic baths at scan rate of 100 mV/sec.	192

Figure 5.17	CVs of Ni-Co alloy electrodeposition recorded at GCE from Ni70%-Co30% bath1 in the presence of 5×10^{-7} M (a) [MOFIM]I; (b) [FPIM]Br with different scan rates. Insert linear relation between i_{cp} as a function of the scan potential rate $v^{1/2}$.	193
Figure 5.18	ALSVs and i_a peaks for Ni-Co alloy electrodeposition from Ni70% - Co30% bath1 in the absence and presence of different concentrations of (a, c) [MOFIM]I; (b, d) [FPIM]Br.	195
Figure 6.1	The optimized molecular structures of (a) [MOFIM]I neutral species, (b) [FPIM]Br neutral species, (c) [MOFIM]I cation species, (d) [FPIM]Br cation species.	204
Figure 6.2	Localization of HOMO of neutral species (a)[MOFIM]I, (b)[FPIM]Br, LUMO of (c)[MOFIM]I and (d)[FPIM]Br. HOMO of cation form (a')[MOFIM]I, (b')[FPIM]Br, LUMO of (c') [MOFIM]I and (d') [FPIM]Br.	206
Figure 6.3	Pictorial representation of mechanism of adsorption of (a) [MOFIM]I, (b) [FPIM]Br on Cu substrate surface. Graphical images of Ni, Co and Ni-Co alloy deposited from bath (c) free-ILs, (d) included [MOFIM]I and [FPIM]Br ILs.	220

LIST OF ABBREVIATIONS

AFM	-	Atomic Force Microscopy
ALSV	-	Anodic Linear Stripping Voltammetry
CCE	-	Cathodic Current Efficiency
CE	-	Counter Electrode
CP	-	Cathodic polarization
CPE	-	Constant phase element
CPP	-	Cathodic Polarization Potential
Cu	-	Copper
CV	-	Cyclic Voltammetry
3D	-	Three Dimensional
2D	-	Two Dimensional
DFT	-	Density Functional Theory
EDX	-	Energy Dispersive X-Ray Spectroscopy
EIS	-	Electrochemical Impedance Spectroscopy Method
E_{HOMO}	-	The highest occupied molecular orbital energy
E_{LUMO}	-	The lowest unoccupied molecular orbital energy
fcc	-	Face Center Cubic
[FPIM]Br	-	1-(4-fluorobenzyl)-3-(4-phenoxybutyl)imidazol-3-ium bromide
GCE	-	Glassy Carbon Electrode
H_{ads}	-	Adsorbed Hydrogen
HER	-	Hydrogen Evolution Reaction
HOMO	-	The highest occupied molecular orbital
ILs	-	Ionic Liquids
LUMO	-	The lowest unoccupied molecular orbital
[MOFIM]I	-	1-methyl-3-((2-oxo-2-(2,4,5 trifluorophenyl) amino)ethyl)-1H-imidazol-3-ium iodide
NOP	-	Nucleation Over Potential
OCP	-	Open-Circuit Potential
Pt	-	Platinum
R_a	-	Average roughness
R_{ct}	-	Charge transfer resistance
RE	-	Reference Electrode
R_s	-	Solution resistance
R_t	-	Total roughness
SCE	-	Saturated Calomel Electrode
SEM	-	Scanning Electron Microscopy
W_{Co}	-	Practical weight of the cobalt deposit
WE	-	Working Electrode

W_{Ni}	-	Practical weight of the nickel deposit
W_p	-	Practical weight of the deposit
W_t	-	Theoretical weight of the deposit
XRD	-	X-Ray Diffraction Analysis

LIST OF SYMBOLS

a	-	Constant
A	-	Electron affinity
A	-	Electrode area
b_c	-	Cathodic tafel slope
C	-	Additive concentration
D	-	Diffusion coefficient
ΔE	-	Energy gap
F	-	Faraday's constant
ΔG°_a	-	Standard free energy of adsorption
I	-	Ionization potential
i	-	Current density in the absence of the additive
i_{add}	-	Current density in the presence of the additive
i_c	-	Cathodic current
i_{pc}	-	Cathodic peak current
K	-	Equilibrium constant of the adsorption reaction
n	-	Number of electrons
ΔN	-	The fraction of electrons transferred from the inhibitor to the metal surface
R	-	The gas constant
S	-	Softness
T	-	Absolute temperature
$v^{1/2}$	-	Proportional to the square root of the scan rate
W	-	Warburg impedance
χ	-	Electronegativity
α_c	-	Electron transfer coefficient
η	-	Hardness
θ	-	Surface coverage
μ	-	Dipole moment

LIST OF APPENDICES

APPENDIX	TITLE	PAGE
Appendix A	Characterization of [MOFIM]I	203
Appendix B	Characterization of [FPIM]Br	207
Appendix C	Molecular Properties and Drug-likeness	211
Appendix D	Tafel Plots and Calculation of Electrochemical Kinetic Parameters	213
Appendix E	Temkin and Flory–Huggins adsorption isotherms	
Appendix F	List of Publications	

CHAPTER 1

INTRODUCTION

1.1 Background of Study

The formation of metallic films and coatings is an important technology and has been applied in many industries. Several coating methods which are commercially available such as vapor deposition, plasma spray, hot metal processes, painting, thermal spraying and metallizing including electrodeposition (1–4) can be used to extend the component's life and protect surface functionality. Ni-Co alloy is commonly produced through electrochemical reduction, leaching process, mechanical alloying, and solgel method (5). Electrodeposition or electroplating is the process by which an applied current or potential is used to deposit a film of metal or alloy by the reduction of metallic ions onto a conductive substrate.

Electroplating finds numerous applications as thin films and three- dimensional, thick structures in micro devices due to its interesting advantages. The main advantages of electrodeposition process are rapid deposition rates, cost effectiveness, requires simpler operating conditions and instrumentation, obtaining a homogenous deposit film. Moreover, many other desirable properties of electrodeposition are simplicity of high level control over the thickness of the films, possible to prepare material that could not be prepared by other methods such as thermal spraying, painting, hot metal processes, and evaporation (1–3). The investigation of more beneficial properties as well as high deposit qualities was conducted using electrodeposition. The deposit exciting qualities are large area deposition, excellent corrosion protection, high strength formability, attractive bright appearance, ease of process ability, and relatively low temperature contrary to the physical systems usually required high temperature (6).

Among the wide range of electroplating materials available, nickel (Ni), cobalt (Co) and Ni-Co alloy are essential engineering material employed widely in several industrial applications. In industrial production, it is usually prepared by means of electrodeposition.

1.2 Properties, Corrosion Resistance and Structure of Nickel, Cobalt and Ni-Co Alloy Electrodeposits:

Nickel (Ni) is silvery-white, hard, malleable, ductile metal and good conductor of heat and electricity. Ni and Ni-based alloy films obtained by electrodeposition approach are widely manufactured to improve the corrosion resistance in engineering application due to their good physical properties, high chemical stability and heat resistance, high current efficiency (>90%) (7) and attractive appearance. Moreover, the appropriate adsorption strength between Ni and adsorbed hydrogen (Ni-H_{ads}) gave Ni deposit high electrocatalysts activity. The addition of additives is considered as responsible for strengthening the passivation phenomenon and enhancing the oxidation resistance of the Ni and its alloy phase in the coating. A reasonable cost of Ni and Ni alloy coatings compared with noble metals makes it an industrially desirable product (8–12). The mechanical properties of Ni deposited are high tensile strength, low ductility, high hardness and high internal strength (13,14).

In electrodeposition technique, mechanic, magnetic, structure and morphological properties of deposits depend on the electrodeposition parameters. The refinement of crystal structure, for example by the use of organic addition agents, is accompanied by increased hardness and tensile strength, and reduced ductility (13,14). The Ni and its alloy coatings which are follow face-centered cubic (fcc) structure, is usually bright, pore-free and crack-free with fine and compact grains coatings. Addition of supporting agent such as Na₂SO₄ to the electrodeposition bath increases the conductivity of the solution, thus facilitating the mass transfer of metal ions towards the cathode surface.

Cobalt (Co) is a hard ferromagnetic, silver-white, lustrous and brittle element. It is stable in air and does not react with water and it can also be magnetized (13,14). The Co properties as good corrosion resistance, high coercivity and high saturation magnetization make Co useful and feasible material for potential applications in magnetic media devices. The special properties of Co electrodeposit, including good strength and thermal stability, high heat conductivity, strong hardness, good resistance to corrosion, good wear resistance, strong adhesion, optical properties, and high catalytic properties (15–17) qualified Co deposit to be very essential engineering material. Co can take two different crystalline structures which are hexagonal closed packed (hcp; ϵ -Co) at $T < 417\text{ }^{\circ}\text{C}$, and fcc; α -Co) at $417\text{ }^{\circ}\text{C} < T < 1493\text{ }^{\circ}\text{C}$ (melting point) (18).

The electrodeposition of iron family-based alloys, including Ni and Co alloy, has been the subject of continuous investigations due to the high magnetic, mechanical chemical, physical and electrocatalytic properties of such coatings (1). Ni-Co alloy possesses an excellent adhesion and wear resistance, good hardness, high corrosion resistance, and heat conductivity. Therefore, Ni-Co alloy coatings are used in various magnetic devices, especially in micro-technology for the manufacture of sensors, actuators, and memory devices (2)(5). The bath composition deposition affects the Ni-Co alloy properties. The cobalt introduction in nickel alloys, $\leq 40\%$, causes an increase in their hardness and strength and corrosion resistance (16)(19).

The bath composition deposition potential and the current density strongly influence the deposit growth mechanism and morphological characterization including surface roughness, microstructure and grain size. If the Ni content is higher than that of Co in the bath, (up to 50wt.%, rich nickel deposit) (2)(20) at high overpotentials, the deposit has lower roughness and finer grain size with face center cubic-close packed structure (fcc) solid solutions of Ni and Co. In contrast, while at low overpotentials, and at higher content of cobalt in the electrolyte (rich cobalt deposit), hexagonal-close packed (hcp) structure, higher surface roughness, bigger grain size of deposits was formed. Moreover Ni-Co alloy deposit with lower Co content exhibits higher hardness and strength (21).

1.3 Mechanism of Ni, Co and Ni-Co alloy electrodeposition

Ni, Co and Ni-Co alloy coatings are constructed using the electrodeposition method through applying the electrical current in the electrochemical cell. The following steps, [Figure 1.1](#), illustrated the mechanism of the formation Ni, Co and Ni-Co alloy electrodeposits from aqueous system (22):

1- The divalent Co and/or Ni ions are surrounded by hydration shells. The solvated ions move towards the negative charged cathode electrode after applying the electrical current on metal substrate cathode.

2- The ions get reduced and neutralized, as the following Eqs. (1.1-1.2):



3- The attractive interaction between water molecule and neutral Co and Ni ions is zero, so hydrated water molecules are displaced and neutral metal atom gives an intermetallic phase according to the following chemical reaction (Eq.1.3 only related to Ni-Co alloy):



4- Then Co and/or Ni diffuse to the surface sites where it incorporates into the metal lattice.

5- After the incorporation into the metal lattice, the Ni, Co and Ni-Co alloy deposits are formed.

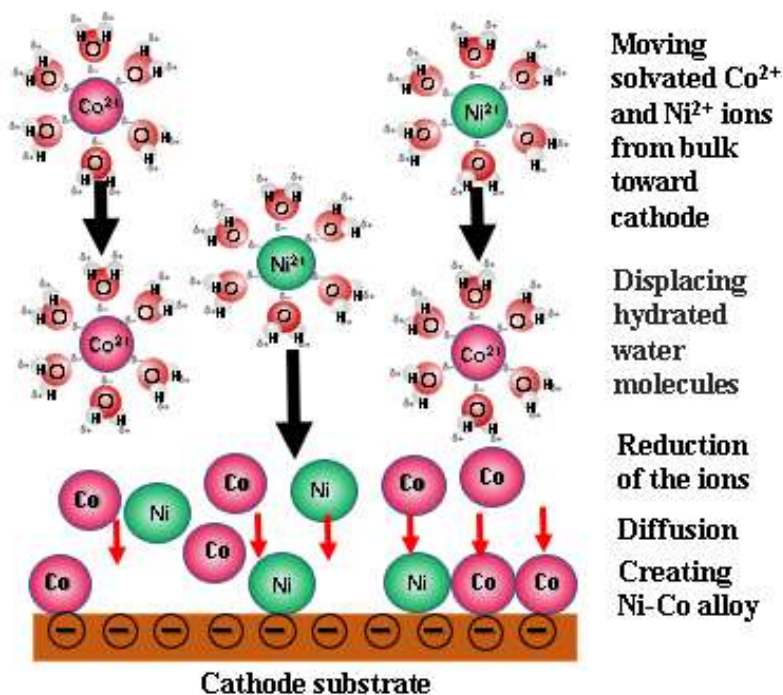


Figure 1.1 Schematic steps illustrated the mechanism of the formation Ni, Co and Ni-Co alloy electrodeposits.

1.4 Applications of Nickel, Cobalt and Ni-Co Alloys in Industry

1.4.1 Application of Nickel

Nickel and nickel alloys are important industrial materials as their wide variety of utilizations, as shown in [Figure 1.1](#). The majority of these applications require heat resistance and high corrosion resistance, (such as nuclear power systems, power stations, steam turbines, and aircraft gas), medical applications, and petrochemical and chemical industries (1–3)(23–25). Being highly resistant to tarnish and high hardness, nickel and nickel alloys have become alternatives for chromium electrodeposition in hardware, automotive, electrical and electronics accessories. Currently, Ni film is considered to be one of the most promising hydrogen evolution reaction (HER) electrocatalysts among high-activity electrocatalysts due to the appropriate adsorption strength between Ni and adsorbed hydrogen (Ni-H_{ads}). Moreover, the significant Ni and its alloy coating properties include stability, high efficiency and reasonable cost of Ni

and Ni alloy coatings compared with noble metals (8–12). Other Ni alloy film applications are in the fabrication of anodes for Li-ion batteries (1–3) and protein microarray fabrication technologies (26). Moreover, because of its favorable mechanical properties, Ni deposits are used for printing, phonography, foils, tubes, screens and many other articles (27).

1.4.2 Application of Cobalt

In engineering, cobalt and its alloys are regarded as essential materials and are commonly used in many industrial applications. This is due to their special characteristics, including good strength and thermal stability, high heat conductivity, strong hardness, good resistance to corrosion, good wear resistance, strong adhesion, optical properties, and high catalytic properties (15–17). Co and its alloys are also used in the manufacture of nanostructural materials such as nanowires and nanotubes and in various storage and magnetic equipment (28). Moreover, Co and its alloys are applied in microsystem technology for the manufacture of sensors, actuators, micro relays, inductors and magnetic devices in the computer industry (16)(29,30), as shown in [Figure 1.1](#). Additionally, it is used in modern accumulators and advanced batteries, as well as in microelectronics for the semiconductor industry (28).

1.4.3 Application of Ni-Co Alloys

Ni-Co alloy deposits are very important due to their industrial applications (such as electronics, computers, automotive and energy storage devices, particularly in the computer field), technological (space, rocketry) applications (1–3)(31,32), biotechnological applications (26) and powerful fabrication applications (33). These significant applications are due to Ni-Co alloys having suitable magnetic, mechanical, chemical, physical and electrocatalytic properties, [Figure 1.1](#). In addition, electrodeposited Ni-Co alloys are widely used as active materials for hydrogen and oxygen evolution reactions in water electrolysis, as anode materials for lithium

batteries, and as catalysts for H₂O₂ decomposition (31)(34). Ni-Co films have been prepared via electrodeposition due to their low cost, easy to maintain equipment, control of film thickness, preparation of high-quality alloys, and capability of handling complex geometries. The method is environmentally friendly compared with other coating technologies including chemical and physical deposition by vapor (1–3).



Figure 1.2 Examples of different Ni, Co and Ni-Co alloy coatings applied on components in various industries.

1.5 Additives in the Electrodeposition Process:

1.5.1 Organic and Inorganic Additives:

The electrodeposition of metals and alloys employed usually by using solutions contain one or more organic or inorganic addition agents which have effective functions

in the electrodeposition processes (35–39). In the aqueous electroplating solutions, it is considerably important to use additives in order to improve the surface morphology of the deposit, produce more precision, durability and stability for coating (40–43), owing mainly to the desirable influences produced on the structure and growth of deposits (44). The increasing in current density range, enhancing potential brightening the deposit, promoting leveling, reducing grain size and the tendency to tree, reducing stress and pitting in the deposited film, and improving physical and mechanical properties, can be achieved by using additives. The additives may even be organic and metallic, ionic and non-ionic, and adsorbed onto the plated surface (6). Organic additives actually seem to enhance the creation of some dominant textures of most crystallites, often inhibiting crystallization process towards the other crystallographic axes (45). These additives influence the processes of deposition and crystal building as adsorbate on the cathode surface (46). The deposit form obtained at a constant current density can depend on the surface coverage value of the additive. Therefore, the adsorbed additives may affect both the kinetics and mechanism of electrodeposition. Organic additives can also elevate surface polarization, increase cathodic overpotential, and suppress the kinetics of electrodeposition reaction (47).

1.5.2 Mechanism of Additives

One of the two main brightener categories is additives. Brighteners are organic or inorganic, ionic or non-ionic compounds that added to the electrodeposition for enhancing the morphological structure of deposit obtained and improving its quality and properties. In aqueous solutions, there are mainly two mechanisms for the brighteners to affect the deposits during the electroplating. One is called leveling agent additive or additive (common name). It is performed by the adsorption of an organic species on the electrode surface, blocking nucleation and hindering growth of metal nucleus. The other is carried through coordinating to the metallic species called complexing agent. Complexing with metal ions leads to decreasing their reduction potential for making it more difficult to nucleate metal clusters (48).

On the other hand, it is important to study the nucleation and growth mechanism of the film structure during electrodeposition. The nucleation mechanism of the conducting metals growth was investigated via the theory model of metal growth (5)(49). The nucleation mechanism includes instantaneous and progressive nucleation was developed by Scharifker and Hills, and the direction of nucleation includes two-dimensional (2-D) and three-dimensional (3-D) growth (5)(49). In an instantaneous nucleation process, the model assumes the rate of nucleation is high and that coverage of all active sites by nuclei, i.e., nucleus grow. In the progressive nucleation mechanism, the rapid growth of a large number of active sites is achieved throughout the reduction, i.e., the number of nuclei increases (5)(44).

The nucleation mechanism of the metal or alloy deposited on the surface is affected significantly by the category of the brighteners used. The leveling agent additive, which is adsorbed on the cathode surface and exhibited the change in the cathodic current density, follows a 3D-progressive nucleation/growth mechanism. The morphology of the deposited metal or alloy is getting leveled (5)(44)(50). However, since the coordination environment of the metal ions in electrodeposition bath was changed by addition of a complexing agent and led to change in the cathodic current density, the electrodeposition of metal or alloy follows a 3D-instantaneous nucleation/growth mechanism (5)(44)(50). With the instantaneous nucleation model, the number of nuclei is constant, and they grow on their former positions on the bare substrate surface without formatting new nuclei. Hence the radii of the nuclei is larger and the surface morphology is rougher. Addition of leveled additive into electrodeposition bath, the nuclei not only grow on their former positions but also on new nuclei, which form smaller nuclei particles and the surface morphology becomes smoother, less granular, flatter and lower roughness (51).

1.6 Ionic Liquids (ILs):

Ionic liquids (ILs) are an interesting challenge for new chemicals with the potential to enhance chemical technology development and stimulating considerable field research. Ionic liquids are organic salts composed of organic cations and

organic/inorganic anions that are liquids at room temperature (39). ILs are synthesized by combining organic cations such as pyridinium, imidazolium, ammonium, phosphonium, and guanidinium with a wide variety of anions including halides (Cl^- , Br^-), hexafluorophosphate (PF_6^-), tetrafluoroborate (BF_4^-), trifluoroacetate (CF_3COO^-), bis-(trifluoromethylsulfonyl) amide (NTf_2), and dicyanamide (DCA) (52). The amount of literature concerning ILs has significantly increased over the past few decades (53). ILs are considered as an efficient alternative to conventional organic solvents. Air and water-stable ILs systems have been emerged because of their unique properties, including such better organic and inorganic solvents, non-volatile, less poisonous, non-flammable, thermal stability (can be used over a wide temperature range up to 400 °C) and negligible vapor pressures (10^{-11} - 10^{-10} mbar) (54). In addition, the most important advantage of ionic liquids is their wide electrochemical windows ($> 5\text{V}$) which offers access to elements which cannot be electrodeposited from aqueous or organic systems (46)(55). Some of the crucial factors that can cause ILs to differ towards aqueous systems are conductivity, viscosity, density, dissolving ability from metal salts, polarity, and potential window. In conclusion, ILs are inevitably sophisticated and advanced solvents which can be formulated to fit the specific application. In addition, eco-sustainable, recyclable material for synthetic organic chemistry, separation sciences and other chemical and engineering sciences have been fully justified for ILs. Due to the multitude of useful properties and abilities of ILs, ILs have now become alternatives for several industrial applications including (54):

- Electrochemistry.
- Synthesis and extraction processes.
- Electrodeposition.
- Liquid crystals.
- Photochemistry.
- Fuel desulfurization.
- CO_2 capture.
- Lubrication.
- Enzymatic synthesis.
- Thermal storage systems.
- Rocket propulsion.

The ionic liquid is defined as an ionic material consists cation and anion with a melting point below 100 °C. Low melting point of ILs arises due to a large, non-symmetrical organic cations and hence low lattice energies of ILs structure (48). It is generally accepted that the cation is more important in controlling the physical properties of the salt whereas the anion has a greater effect upon the stability and chemical reactivity. The majority of ILs systems used for metal deposition have been based on nitrogen-based cations. Imidazolium based cations, which are chosen in the current work, have been favored due to their superior fluidity and conductivity. The other important role that the cation probably plays in electrodeposition is controlling the structure and most importantly the Helmholtz layer thickness. Anions also affect the conductivity and viscosity of the electrolyte. Anions could decrease the Helmholtz layer thickness considerably and should make metal ion reduction easier (48).

1.6.1 Ionic Liquid as Additives

Due to special properties of ionic liquids, such as undetectable vapor pressure, a wide range of liquids, fast recovery and reuse, ionic liquids are a strong alternative to traditional molecular organic solvents in recent years (53). Scientists are currently interested in ionic liquids applications, including imidazolium-ionic liquids as additives (36). Ionic liquids reporting in the liquid chromatography (56), sustainable solutions (57), organic synthesis, catalytic reactions, and ILs used as lubricants and corrosion inhibitors (53).

1.7 Quantum Chemical Calculation:

The investigation of ionic liquid additives performance in the electrodeposition processes are conducted experimentally. In addition, computational chemistry can be used to provide theoretical explanation for the experimental findings. Experimental measurements to achieve the effect of ionic liquid as additives in Ni, Co and Ni-Co alloy electrodeposition process are conducted using various techniques which are

studied deeply in the experimental section. Traditionally, experimental techniques are mainly used to investigate the additives performance in the electrodeposition field. However, employing the experimental methods only is harmful to the environment, expensive and time consuming (58). With the improvement in computer hardware and software as well as in theoretical chemistry, computational chemistry has been increasingly used in the design and development of addition agents in the electrodeposition field (43)(59–61) and corrosion inhibitors (58)(62–65). As reported in (59) "Density functional theory (DFT) has become an active field of research to envisage the mechanism arising between additives and surface of the metal at the molecular level".

1.8 Problem Statement

An organic or inorganic compound is considered as one of the main components of electrodeposition solution of single metal or alloy due to a positive and beneficial effects of specific functions of additives on the deposit's properties. Adding additives in Ni, Co and Ni-Co alloy electrodepositions processes is not very common. Moreover, glycine, acetonitrile and choline chloride–urea (1:2 molar ratio) which were used as additives in the Ni-Co alloy electrodeposition exhibits granular, no uniform deposits (1)(66–68). An extensive micro-cracked deposits were produced by adding glycine, thiourea, sodium gluconate, boric acid, coumarin and saccharin due to hydrogen evolution (23,24)(15)(59–62). Non-brightness, low corrosion resistance Ni-Co alloy deposit obtained by using nano Al_2O_3 particles as additive (32). Moreover, the hardness and the strength of deposits (27)(16) and the cathodic current efficiency (CCE%) of some studies were very low (15)(36)(39,40). Insufficient thermal stability and poor throwing power were achieved in other studies (23)(27)(7).

In addition, Ni, Co and Ni-Co alloy crack free films were produced in the presence of glycine and sodium citrate (67)(69) as additives but these studies required high temperature and high current density. Moreover, some studies used an expensive substrate such as gold, Pt, Si (25)(29)(66). The others consumed high concentration of

metal sources and additives (16)(29)(66). Some studies used non environmentally friendly, toxic such as Cd^{2+} (70) and cyanides (71), highly flammable and volatile substances, acetone, (50) and health hazards substance, thiourea (50), as additives. Moreover, some works lack for hardness and corrosion resistance measurements (36)(72–74).

Ionic liquids have been applied as a media of electrodeposition process by many researchers (24)(34)(50,51)(67)(75) but some of them obtained micro-cracked, granular films, and low CCE% (24)(31)(44)(46) (50,51)(67,68). However, using ionic liquids as addition agents in the electrodeposition processes attracted only few researchers (39)(53). This means that study the effect of ILs as additives during electrodeposition process is insufficient.

Many investigations into Ni induced from different baths including, sulfamate, chloride, citrate, acetate, gluconate, glycine, and Watts-type nickel electrodeposition bath, without or with additives were recorded (76–78). Moreover, cobalt deposits has been obtained from different baths containing chloride (79), chloride & sulfate (80), gluconate (81), acetate (82) and citrate (83) electrolytes. Unfortunately, some of these coating deposited in industry from electrolytic baths contains toxic solutions such as the cyanide anions (71)(84). A distinguished feature of cyanide-based systems is obtained fixable and soft deposits, strong adhere to alloys, good electrical conductivity, easily buffed, good solderability and obtaining decorative, bright and attractive antique finishes (84). Cyanide process is being prohibited due to its health and environmental pollution hazards as well as high cost involved to treat the effluent. Therefore, demanding to use green and more environmentally friendly electrolytes in the industrial fields become extremely necessary to decrease the problem of pollution in the world. Using acid sulfate bath is attracted many attentions due to pollution control characteristics, its safety features and relatively low cost (85). Moreover, finer grained and smoother surface was obtained from sulfate bath than that which was obtained from other baths (38).

On the other hand, employing experimental approaches only for investigating the additive's role in the electrodeposition is not eco-friendly, costly and time

consuming. Therefore, applying computational techniques, including quantum chemical calculations as predictive techniques, is more environmentally friendly, time saver and more economic (64). The practical investigations are complemented through computational systems. These systems are effective tools to propose the effective ionic liquids as additive among an enormous group of additives using in the electroplating field. Quantum chemical calculations are used to support the experimental investigations. Al-Fakih et al (64) reported that "Density functional theory (DFT) is a quantum chemical approach that is considered a powerful tool to investigate the quantum parameters of molecules theoretically with reasonable accuracy". Moreover, the natural atomic charge, i.e., Mulliken population analysis, has been calculated to determine the active sites and the adsorption mode of additives or inhibitor molecules, which can offer or accept electrons (86). As reported in (86) "There is a general consensus that the more negatively charged the heteroatom is, the more adsorption centers there are on the metal surface through donor–acceptor interactions". The use of Mulliken population analysis has been widely reported for calculation of the charge distribution over the whole skeleton of inhibitor molecules (64)(59).

Most of studies which used the quantum chemical parameters were conducted for organic compounds as additives in the electrodeposition field (43)(59) (60,61)(87) or as corrosion inhibitors (62)(64)(86)(88). Moreover, many other researchers calculated the natural atomic charge and determined the active sites and the adsorption mode of organic compounds as corrosion inhibitors (62)(64) or as additive in the electrodeposition (59).

Although some studies used ionic liquids as electrodeposition electrolytes (72)(89) or as corrosion inhibitors (90,91). However, very limited studies have used the quantum chemical parameters for clarifying the behavior of ionic liquids which are used as additives during the electrodeposition processes. It could be said that the studies regarding the use of quantum chemical calculations on ionic liquid compounds as additive in Ni, Co and Ni-Co alloy electroplating are not many and very poor.

According to the gaps in all previous research in the Ni, Co and their alloys electrodeposition, the main aim of the current study is improving the qualities of Ni, Co

and Ni-Co alloys deposits by investigating the influence of two new green eco-friendly imidazolium ionic liquids using as addition agents in the electrodeposition of Ni, Co and Ni-Co alloy from acidic baths.

Furthermore, in the current work, the quantum chemical calculations as theoretical tools are used to explain the adsorption performance of two studied ionic liquids additives based on their molecular structure properties. Moreover, electronic properties and molecule orbital information were obtained by quantum chemical calculation to further analyze the interaction between studied ionic liquid and metal surface. In addition, the natural atomic charge was calculated and employed to investigate the active sites of two imidazole derivatives ionic liquids molecules which can offer or accept electrons.

1.9 Research Objectives

As stated by all previous research gaps, obtaining Ni, Co and its alloy via electrodeposition by applying a novel green ILs become very essential to achieve it in current study. Therefore, the objectives of the present study are as follows:

1. To study the electrodeposition of Ni, Co and Ni-Co alloy in the absence and the presence of [MOFIM]I and [FPIM]Br ionic liquids as new additives.
2. To characterize the surface morphology and microstructure of Ni, Co and Ni-Co alloy deposits in the presence of the studied new ionic liquids as additives from acidic sulfate bath.
3. To optimize the ionic liquids as additives in the electrodeposition of Ni, Co and Ni-Co alloy by using density functional theory (DFT).
4. To study the structure and properties relationship of Ni, Co and Ni-Co alloy deposits prepared by electrodeposition with the presence of the studied new ionic liquids.

1.10 Scope of the Research

Figure 1.3. illustrated the molecular structure of two new studied ionic liquids namely:

- 1- Imidazolium iodide incorporating aromatic amide (name: 1-methyl-3-(2-oxo-2-((2,4,5trifluorophenyl)amino)ethyle)-1H-imidazol-3-ium iodide [MOFIM]I ionic liquid.
- 2- Imidazolium bromide (name: 1-(4-fluorobenzyl)-3-(4-phenoxybutyl)imidazol-3-ium bromide [FPIM]Br ionic liquid.

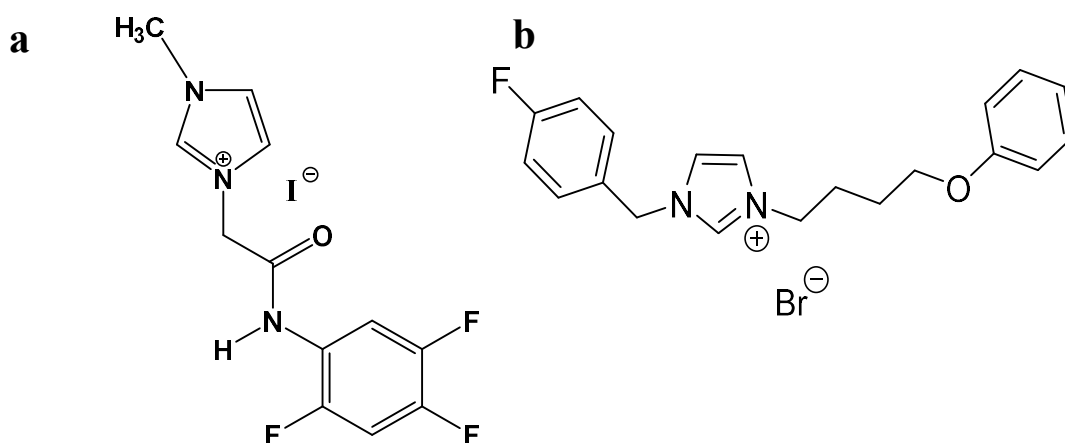


Figure 1.3 The molecular structure of the ionic liquids namely (a) 1-methyl-3-(2-oxo-2-((2,4,5 trifluorophenyl) amino) ethyl)-1 imidazol-3-ium iodide ([MOFIM]I), (b) 1-(4-fluorobenzyl)- 3-(4-phenoxybutyl)imidazol-3-ium bromide ([FPIM]Br).

The effect of many important factors will be studied in the electrodeposition of Ni, Co and Ni-Co alloy. The first factor is concentrations of two studied ILs in the range from 1×10^{-7} to 1×10^{-3} M, The other factors that will be studied in the electrodeposition of Ni, Co and Ni-Co alloy are including pH, in the range from 3.5 to 4.5, electroplating time, in the range from 5 to 15 min, current density, in the range from 6 to 24 mA/cm², and electroplating potential, in the range from 3 to 9 V. Three different bath compositions for co-electrodeposition of Ni-Co alloy, as illustrated in Table 3.2 in chapter 3, will be investigated. These selected range of all previous factors are due to

the best coating qualities and high cathodic current efficiency (CCE%) are obtained, as reported in (1)(3)(15)(7)(49). Moreover, the CCE% during electrodeposition processes will be investigated at all these factors.

Characterization the surface morphology, elemental compositions, roughness, microstructure and microhardness of Ni, Co and Ni-Co alloys deposited in the absence and the presence of two studied ILs will be obtained by using microscopic analysis such as scanning electron microscopy (SEM), energy dispersive X-ray spectrometry (EDX), EDX mapping, atomic force microscopy (AFM) and X-ray diffraction analysis (XRD). Moreover, the mechanical properties such as micro-hardness of Ni, Co and Ni-Co alloy deposits will be measured.

The mechanism of the electroplating process of Ni, Co and Ni-Co alloys in absence and presence of additives will be achieved experimentally by using voltametric analysis such as (potentiodynamic cathodic polarization curves, cyclic voltammetry (CV), In situ-anodic linear stripping voltammetry (ALSV)). The electrochemical corrosion behavior in a saline environment (3.5% NaCl solution) will be investigated using potentiodynamic polarization and electrochemical impedance spectroscopy (EIS) techniques.

Optimization of the neutral and cationic forms of both [MOFIM]I and [FPIM]Br ionic liquids used as additives in the electrodeposition of Ni, Co and Ni-Co alloy will be investigated by using quantum chemical calculations. Quantum chemical calculations using DFT was conducted to calculate quantum parameters and discuss the relationship with the experimental findings. Several quantum parameters, such as highest occupied molecular orbital energy (E_{HOMO}), lowest unoccupied molecular orbital energy (E_{LUMO}), energy gap (ΔE), ionization potential (I), electron affinity (A), electronegativity (χ), hardness (η), softness (S) and fraction of electrons transferred (ΔN), and the natural atomic charge will be calculated using DFT (44). The results of the quantum chemical calculations will be served as a theoretical confirmation for the experimental data based on the quantum chemistry of the ionic liquids molecules.

1.11 Significance of the Study

In the current study, two new [MOFIM]I and [FPIM]Br ionic liquids will be added in Ni, Co and Ni-Co alloy electroplating baths to enhance the qualities, the surface morphology, hardness and the corrosion resistance of Ni, Co and Ni-Co alloy deposits. It is hopeful to overcome these defects of traditional additives and toxic organic corrosion inhibitors and help to realize additives with good stability and inhibitors with a virulence by using ILs as metal electrodeposition additives and corrosion inhibitors, respectively. This study will provide our industry with new ionic liquids for producing good quality Ni-Co alloy deposits from environmentally friendly solutions.

The use of quantum chemical calculations in this study complements the experimental measurements. The calculations provide theoretical descriptions for the effect of ionic liquid behavior on structures and mechanical properties of Ni, Co and Ni-Co alloy. The implementation of these procedures is useful to predict potential efficient ionic liquids additives, and thus will reduce the cost and time of testing inefficient ionic liquids. Based on our research, quantum chemical calculations are used effectively for the prediction of ionic liquids as addition agents in Ni, Co and Ni-Co alloy electroplating. This efficient and versatile method thus opens a new window to study or design ionic liquids for generalized metal electroplating and will vigorously promote the level of this research region.

1.12 Outline of the Thesis

The dissertation is split into seven chapters. **Chapter 1** provides a summary of the research, a brief history on the advantages of the electrodeposition process, the applications of industrial deposits of Ni, Co and Ni-Co alloys, the mechanism of Ni, Co and Ni-Co alloy electrodeposition, the effective role of additives in improving the consistency of deposited films, the advantages of using ionic liquid as additives in the field of electrodeposition and experimental measurement methods, and theoretical

approaches. It also includes the present study's problem statement, aims, importance and scope. The related literature of the present study is discussed in **Chapter 2**. The literature was reviewed on the basis of four key subjects, previous studies in electrodeposition of Ni, Co and Ni-Co alloys, organic compounds as additives, mechanism of additives in the electrodeposition, the nucleation mechanism of deposit, ionic liquid including synthesis, description, structure, properties and utilities of electrodeposition processes, mechanism of Ni, Co and Ni-Co alloy electrodeposition in the presence of ionic liquid as additive, the principle of adsorption isotherm and quantum chemical calculations of additives and corrosion inhibitors. The details and specifics of the experimental methods are given in **Chapter 3**. An overview of the key experimental procedures used to investigate the current efficiency, voltametric behavior and mechanism, surface morphology, hardness and corrosion resistance of deposited Ni, Co and Ni-Co alloys from acidic baths is included. The findings result from the experimental work, discussion, and derived conclusions are discussed. **Chapter 4** is split into two sections (A and B). The findings and discussion of the Co and Ni electrodeposition measurements in the absence and presence of different concentrations of [MOFIM]I and [FPIM]Br were included in both sections. **Chapter 5** describes the outcomes and discussion of the Ni-Co alloy electrodeposition experimental study with three primary compositions of Ni²⁺ and Co²⁺ ions without and with [MOFIM]I and [FPIM]Br. Then, the main results are presented from all experimental measurements. The details of the quantum chemical calculation are given in **Chapter 6**. An overview of the procedures used and the quantum parameters measured and the natural atomic charge is given. The key conclusions of the present work and a brief description of this study are given in **Chapter 7** and some suggestions for future work are provided.

REFERENCES

1. Radadi RM Al, Ibrahim MAM. Nickel-cobalt alloy coatings prepared by electrodeposition Part I : Cathodic current efficiency , alloy composition , polarization behavior and throwing power. *Korean J Chem Eng.* 2020;37(2):1–10.
2. Al Radadi RM, Ibrahim MAM. Nickel-cobalt alloy coatings prepared by electrodeposition Part II: Morphology, structure, microhardness, and electrochemical studies. *Korean J Chem Eng.* 2021;38(1):152–62.
3. Al Raddadi RM. Cathodic codeposition of nickel-cobalt alloy coatings from acidic glycine complex baths. MSc Thesis.Taibah university; 2014.
4. Liu F, Deng Y, Han X, Hu W, Zhong C. Electrodeposition of metals and alloys from ionic liquids. *J Alloys Compd.* 2016;654:163–70.
5. Li W, Hao J, Mu S, Liu W. Electrochemical behavior and electrodeposition of Ni-Co alloy from choline chloride-ethylene glycol deep eutectic solvent. *Appl Surf Sci.* 2020;507:144889.
6. Omar EMA. Effect of Organic Additives on Zinc Electrodeposition from Acidic Sulfate Bath. MSc Thesis.Taibah University; 2012.
7. Ibrahim MAM, Al Radadi RM. Role of glycine as a complexing agent in nickel electrodeposition from acidic sulphate bath. *Int J Electrochem Sci.* 2015;10(6):4946–71.
8. Zhao X, Shang X, Quan Y, Dong B, Han G-Q, Li X, et al. Electrodeposition-solvothermal access to ternary mixed metal Ni-Co-Fe sulfides for highly efficient electrocatalytic water oxidation in alkaline media. *Electrochim Acta.* 2017;230:151–9.
9. Wang J, Wang Y, Xie T, Deng Q. Facile and fast synthesis of Ni composite coating on Ti mesh by electrodeposition method for high-performance hydrogen production. *Mater Lett.* 2019;245:138–41.
10. Wu Y, Gao Y, He H, Zhang P. Electrodeposition of self-supported Ni–Fe–Sn film on Ni foam: An efficient electrocatalyst for oxygen evolution reaction. *Electrochim Acta.* 2019;301:39–46.
11. Yao K, Zhai M, Ni Y. α -Ni (OH) 2 · 0.75 H₂O nanofilms on Ni foam from simple NiCl₂ solution: Fast electrodeposition, formation mechanism and

- application as an efficient bifunctional electrocatalyst for overall water splitting in alkaline solution. *Electrochim Acta*. 2019;301:87–96.
12. Liu H, Zeng S, He P, Dong F, He M, Zhang Y, et al. Samarium oxide modified Ni-Co nanosheets based three-dimensional honeycomb film on nickel foam: A highly efficient electrocatalyst for hydrogen evolution reaction. *Electrochim Acta*. 2019;299:405–14.
 13. Zentner V. Discussion of “The Influence of Residual Stress on the Magnetic Characteristics of Electrodeposited Nickel and Cobalt” [RD Fisher (pp. 479–485, Vol. 109, No. 6)]. *J Electrochem Soc*. 1962;109(12):1221.
 14. Safranek WH. *The Properties of Electrodeposited Metals and Alloys: a Handbook*. Am Electroplat Surf Finish Soc 1986,. 1986;550.
 15. Ibrahim MAM, Al Radadi RM. Noncrystalline cobalt coatings on copper substrates by electrodeposition from complexing acidic glycine baths. *Mater Chem Phys*. 2015;151:222–32.
 16. Zamani M, Amadeh A, Baghal SML. Effect of Co content on electrodeposition mechanism and mechanical properties of electrodeposited Ni–Co alloy. *Trans Nonferrous Met Soc China*. 2016;26(2):484–91.
 17. Barrera E, Pardavé MP, Batina N, González I. Formation mechanisms and characterization of black and white cobalt electrodeposition onto stainless steel. *J Electrochem Soc*. 2000;147(5):1787–96.
 18. Karimzadeh A, Aliofkhazraei M, Walsh FC. A review of electrodeposited Ni-Co alloy and composite coatings: Microstructure, properties and applications. *Surf Coatings Technol*. 2019;372:463–98.
 19. Danilov FI, Samofalov VN, Sknar I V, Sknar YE, Baskevich AS, Tkach IG. Structure and properties of Ni—Co alloys electrodeposited from methanesulfonate electrolytes. *Prot Met Phys Chem Surfaces*. 2015;51(5):812–6.
 20. Kharmachi I, Dhouibi L, Berçot P, El M R. Co-deposition of Ni-Co alloys on carbon steel and corrosion resistance. *J Mater Environ Sci*. 2015;6(7):1807–12.
 21. Rafailović LD, Artner W, Nauer GE, Minić DM. Structure, morphology and thermal stability of electrochemically obtained Ni–Co deposits. *Thermochim Acta*. 2009;496(1–2):110–6.
 22. Mukhtar A, Mehmood T, Wu KM. Investigation of phase transformation of CoNi alloy nanowires at high potential. In: *IOP Conference Series: Materials*

- Science and Engineering. IOP Publishing; 2017. p. 12017.
23. El Rehim SSA, Ibrahim MAM, Dankeria MM. Electrodeposition of cobalt from gluconate electrolyte. *J Appl Electrochem.* 2002;32(9):1019–27.
 24. Fukui R, Katayama Y, Miura T. The effect of organic additives in electrodeposition of Co from an amide-type ionic liquid. *Electrochim Acta.* 2011;56(3):1190–6.
 25. Oliveira EM, Finazzi GA, Carlos IA. Influence of glycerol, mannitol and sorbitol on electrodeposition of nickel from a Watts bath and on the nickel film morphology. *Surf coatings Technol.* 2006;200(20–21):5978–85.
 26. Chang Y-J, Chen S-Z, Ho C-Y. Crystallographic structure of Ni–Co coating on the affinity adsorption of histidine-tagged protein. *Colloids Surfaces B Biointerfaces.* 2015;128:55–60.
 27. Ibrahim MAM, El Rehim SSA, El Wahaab SMA, Dankeria MM. Nickel electroplating on steel from acidic citrate baths. *Plat Surf Finish.* 1999;86(4):69–75.
 28. Dragos-Pinzaru O, Ghemes A, Chiriac H, Lupu N, Grigoras M, Riemer S, et al. Magnetic properties of CoPt thin films obtained by electrodeposition from hexachloroplatinate solution. Composition, thickness and substrate dependence. *J Alloys Compd.* 2017;718:319–25.
 29. Manhabosco TM, Müller IL. Influence of saccharin on morphology and properties of cobalt thin films electrodeposited over n-Si (100). *Surf Coatings Technol.* 2008;202(15):3585–90.
 30. Santos JS, Matos R, Trivinho-Strixino F, Pereira EC. Effect of temperature on Co electrodeposition in the presence of boric acid. *Electrochim Acta.* 2007;53(2):644–9.
 31. Zhu Y-L, Katayama Y, Miura T. Effects of acetonitrile on electrodeposition of Ni from a hydrophobic ionic liquid. *Electrochim Acta.* 2010;55(28):9019–23.
 32. Cârâc G, Ispas A. Effect of nano-Al₂O₃ particles and of the Co concentration on the corrosion behavior of electrodeposited Ni–Co alloys. *J Solid State Electrochem.* 2012;16(11):3457–65.
 33. Grill CD, Kollender JP, Hassel AW. Electrodeposition of cobalt–nickel material libraries. *Phys status solidi.* 2015;212(6):1216–22.
 34. Yang P, Zhao Y, Su C, Yang K, Yan B, An M. Electrodeposition of Cu–Li alloy from room temperature ionic liquid 1-butyl-3-methylimidazolium

- tetrafluoroborate. *Electrochim Acta*. 2013;88:203–7.
35. Jamil Z, Ruiz-Trejo E, Brandon NP. Nickel Electrodeposition on Silver for the Development of Solid Oxide Fuel Cell Anodes and Catalytic Membranes. *J Electrochem Soc*. 2017;164(4):210–7.
 36. Allahyarzadeh MH, Roozbehani B, Ashrafi A. Electrodeposition of high Mo content amorphous/nanocrystalline Ni–Mo alloys using 1-ethyl-3-methylimidazolium chloride ionic liquid as an additive. *Electrochim Acta*. 2011;56(27):10210–6.
 37. Fashu S, Gu C, Zhang J, Huang M, Wang X, Tu J. Effect of EDTA and NH₄Cl additives on electrodeposition of Zn–Ni films from choline chloride-based ionic liquid. *Trans Nonferrous Met Soc China*. 2015;25(6):2054–64.
 38. El-Feky H, Negem M, Roy S, Helal N, Baraka A. Electrodeposited Ni and Ni-Co alloys using cysteine and conventional ultrasound waves. *Sci China Chem*. 2013;56(10):1446–54.
 39. Qibo Z, Yixin H. Ionic Liquids as Electrodeposition Additives and Corrosion Inhibitors. In: *Progress and Developments in Ionic Liquids*. InTech; 2017.
 40. Oishi T, Yaguchi M, Koyama K, Tanaka M, Lee J. Effect of additives on monovalent copper electrodeposition in ammoniacal alkaline solutions. *Hydrometallurgy*. 2013;133:58–63.
 41. Sorour N, Zhang W, Ghali E, Houlachi G. A review of organic additives in zinc electrodeposition process (performance and evaluation). *Hydrometallurgy*. 2017;171:320–32.
 42. Song Y, Tang J, Hu J, Yang H, Gu W, Fu Y, et al. Interfacial assistant role of amine additives on zinc electrodeposition from deep eutectic solvents: an in situ X-ray imaging investigation. *Electrochim Acta*. 2017;240:90–7.
 43. Deng J, Zhang J, Tu Y, Yang P, An M, Wang P. Effect of BEO in the electrodeposition process of Ni/diamond composite coatings for preparation of ultra-thin dicing blades: Experiments and theoretical calculations. *Ceram Int*. 2018;44(14):16828–36.
 44. Alesary HF, Cihangir S, Ballantyne AD, Harris RC, Weston DP, Abbott AP, et al. Influence of additives on the electrodeposition of zinc from a deep eutectic solvent. *Electrochim Acta*. 2019;304:118–30.
 45. Hamilakis S, Balgis D, Milonakou-Koufoudaki K, Mitzithra C, Kollia C, Loizos Z. Electrodeposition of CdSe photoabsorber thin films in the presence

- of selected organic additives. *Mater Lett.* 2015;145:11–4.
46. Ibrahim S, Bakkar A, Ahmed E, Selim A. Effect of additives and current mode on zinc electrodeposition from deep eutectic ionic liquids. *Electrochim Acta.* 2016;191:724–32.
 47. Hashemi AB, Kasiri G, La Mantia F. The effect of polyethyleneimine as an electrolyte additive on zinc electrodeposition mechanism in aqueous zinc-ion batteries. *Electrochim Acta.* 2017;258:703–8.
 48. Abbott AP, McKenzie KJ. Application of ionic liquids to the electrodeposition of metals. *Phys Chem Chem Phys.* 2006;8(37):4265–79.
 49. El Sayed MA, Ibrahim MAM. Natural Kermes Dye as an Effective Additive for Electrochemical Deposition of Nickel from Watts-type Nickel Bath. *Int J Electrochem Sci.* 2019;14:4957–73.
 50. Zhu Y-L, Katayama Y, Miura T. Effects of acetone and thiourea on electrodeposition of Ni from a hydrophobic ionic liquid. *Electrochim Acta.* 2012;85:622–7.
 51. Zhu Y-L, Katayama Y, Miura T. Effects of coumarin and saccharin on electrodeposition of Ni from a hydrophobic ionic liquid. *Electrochim Acta.* 2014;123:303–8.
 52. Rezki N, Al-blewi FF, Al-Sodies SA, Alnuzha AK, Messali M, Ali I, et al. Synthesis, Characterization, DNA Binding, Anticancer, and Molecular Docking Studies of Novel Imidazolium-Based Ionic Liquids with Fluorinated Phenylacetamide Tethers. *ACS Omega.* 2020;
 53. Ibrahim MAM, Messali M. Ionic Liquid [BMPy] Br as an effective additive during Zinc electrodeposition from an aqueous Sulfate bath. *Nasf Surf Technol Finish.* 2011;2:182–90.
 54. Tian G-C, Zhou X-J, Jian LI, Hua Y-X. Quantum chemical aided molecular design of ionic liquids as green electrolytes for electrodeposition of active metals. *Trans Nonferrous Met Soc China.* 2009;19(6):1639–44.
 55. Anicai L, Florea A, Visan T. Studies regarding the nickel electrodeposition from choline chloride based ionic liquids. In: *Applications of Ionic Liquids in Science and Technology.* InTech; 2011.
 56. Polyakova Y, Row KH. Retention behaviour of N-CBZ-D-phenylalanine and D-tryptophan: effect of ionic liquid as mobile-phase modifier. *Acta Chromatogr.* 2006;17:210–21.

57. Messali M. A green microwave-assisted synthesis, characterization and comparative study of new pyridinium-based ionic liquids derivatives towards corrosion of mild steel in acidic environment. *J Mater Environ Sci*. 2011;2(2):174–85.
58. AL-FAKIH AMALI. EXPERIMENTAL AND COMPUTATIONAL STUDIES OF FURAN DERIVATIVES IN CORROSION INHIBITION OF MILD STEEL. Ph.D.thesis.Universiti Teknologi Malaysia; 2017.
59. Kumar UP, Shanmugan S, Kennady CJ, Shibli SMA. Anti-corrosion and microstructural properties of Ni–W alloy coatings: effect of 3, 4-Dihydroxybenzaldehyde. *Heliyon*. 2019;5(3):1–27.
60. Liu A, Ren X, An M, Zhang J, Yang P, Wang B, et al. A combined theoretical and experimental study for silver electroplating. *Sci Rep*. 2014;4(1):1–10.
61. Ren S, Lei Z, Wang Z. Investigation of nitrogen heterocyclic compounds as levelers for electroplating cu filling by electrochemical method and quantum chemical calculation. *J Electrochem Soc*. 2015;162(10):D509–14.
62. Murulana LC, Kabanda MM, Ebenso EE. Investigation of the adsorption characteristics of some selected sulphonamide derivatives as corrosion inhibitors at mild steel/hydrochloric acid interface: Experimental, quantum chemical and QSAR studies. *J Mol Liq*. 2016;215:763–79.
63. Lukovits I, Kalman E, Zucchi F. Corrosion inhibitors—correlation between electronic structure and efficiency. *Corrosion*. 2001;57(1):3–8.
64. Al-Fakih AM, Abdallah HH, Aziz M. Experimental and theoretical studies of the inhibition performance of two furan derivatives on mild steel corrosion in acidic medium. *Mater Corros*. 2019;70(1):135–48.
65. Al-Fakih AM, Abdallah HH, Maarof H, Aziz M. Experimental and quantum chemical calculations on corrosion inhibition of mild steel By two furan derivatives. *J Teknol*. 2016;78(6–12):121–5.
66. Ji X, Yan C, Duan H, Luo C. Effect of phosphorous content on the microstructure and erosion–corrosion resistance of electrodeposited Ni-Co-Fe-P coatings. *Surf Coatings Technol*. 2016;302:208–14.
67. Guo J, Guo X, Wang S, Zhang Z, Dong J, Peng L, et al. Effects of glycine and current density on the mechanism of electrodeposition, composition and properties of Ni–Mn films prepared in ionic liquid. *Appl Surf Sci*. 2016;365:31–7.

68. Wang S, Guo X, Yang H, Dai J, Zhu R, Gong J, et al. Electrodeposition mechanism and characterization of Ni–Cu alloy coatings from a eutectic-based ionic liquid. *Appl Surf Sci.* 2014;288:530–6.
69. Lupi C, Dell’Era A, Pasquali M. Effectiveness of sodium citrate on electrodeposition process of NiCoW alloys for hydrogen evolution reaction. *Int J Hydrogen Energy.* 2017;42(48):28766–76.
70. Mohanty US, Tripathy BC, Singh P, Das SC. Effect of Cd²⁺ on the electrodeposition of nickel from sulfate solutions. Part I: Current efficiency, surface morphology and crystal orientations. *J Electroanal Chem.* 2002;526(1–2):63–8.
71. Mizuhashi S, Arakawa T, Watanabe N, Koike S, Urano M, Maejima K, et al. Cyanide Detection from Nickel Electrodeposited in Modified Watts Baths Including Glycine and Cyanide Production at Anodic Sides in the Baths. *Electrochemistry.* 2016;84(6):394–7.
72. Abebe A, Admassie S, Villar-Garcia IJ, Chebude Y. 4, 4-Bipyridinium ionic liquids exhibiting excellent solubility for metal salts: Potential solvents for electrodeposition. *Inorg Chem Commun.* 2013;29:210–2.
73. Zhang Q, Hua Y. Kinetic investigation of zinc electrodeposition from sulfate electrolytes in the presence of impurities and ionic liquid additive [BMIM] HSO₄. *Mater Chem Phys.* 2012;134(1):333–9.
74. Carlesi C, Cortes E, Dibernardi G, Morales J, Muñoz E. Ionic liquids as additives for acid leaching of copper from sulfidic ores. *Hydrometallurgy.* 2016;161:29–33.
75. Vijayakumar J, Mohan S, Kumar SA, Suseendiran SR, Pavithra S. Electrodeposition of Ni–Co–Sn alloy from choline chloride-based deep eutectic solvent and characterization as cathode for hydrogen evolution in alkaline solution. *Int J Hydrogen Energy.* 2013;38(25):10208–14.
76. Wojciechowski J, Baraniak M, Pernak J, Lota G. Nickel Coatings Electrodeposited from Watts Type Baths Containing Quaternary Ammonium Sulphate Salts. *Int J Electrochem Sci.* 2017;3350–60.
77. Schmitz EPS, Quinaia SP, Garcia JR, de Andrade CK, Lopes MC. Influence of commercial organic additives on the nickel electroplating. *Int J Electrochem Sci.* 2016;11:983–97.
78. El Boraie NF, Ibrahim MAM. Catalytic effect of l-proline on the reduction of

- Ni (II) ions during nickel electrodeposition from a Watts-type nickel bath. *Surf Coatings Technol.* 2018;347:113–22.
79. Sivaraman KM, Ergeneman O, Pané S, Pellicer E, Sort J, Shou K, et al. Electrodeposition of cobalt–yttrium hydroxide/oxide nanocomposite films from particle-free aqueous baths containing chloride salts. *Electrochim Acta.* 2011;56(14):5142–50.
 80. Tian L, Xu J, Xiao S. The influence of pH and bath composition on the properties of Ni–Co coatings synthesized by electrodeposition. *Vacuum.* 2011;86(1):27–33.
 81. Abd El Rehim SS, Ibrahim MAM, Dankeria MM, Emad M. Electrodeposition of amorphous cobalt-manganese alloys on to steel from gluconate baths. *Trans IMF.* 2002;80(3):105–9.
 82. Nemțoi G, Chiriac H, Dragoș O, Apostu M-O, Lutic D. The voltammetric characterization of the electrodeposition of cobalt, nickel and iron on gold disk electrode. *Acta Chem Iasi.* 2009;17:151–68.
 83. Abd El Rehim SS, Abd El Wahaab SM, Ibrahim MAM, Dankeria MM. Electroplating of cobalt from aqueous citrate baths. *J Chem Technol Biotechnol Int Res Process Environ Clean Technol.* 1998;73(4):369–76.
 84. Horner J. Cyanide Copper Plating. *Plat Surf Finish.* 1995;82(8):53–6.
 85. Loto CA. Electrodeposition of zinc from acid based solutions: a review and experimental study. *Asian J Appl Sci.* 2012;5(6):314–26.
 86. El-Raouf MA, Khamis EA, Kana MTHA, Negm NA. Electrochemical and quantum chemical evaluation of new bis (coumarins) derivatives as corrosion inhibitors for carbon steel corrosion in 0.5 M H₂SO₄. *J Mol Liq.* 2018;255:341–53.
 87. Liao C, Zhang S, Chen S, Qiang Y, Liu G, Tang M, et al. The effect of tricyclazole as a novel leveler for filling electroplated copper microvias. *J Electroanal Chem.* 2018;827:151–9.
 88. Sulaiman KO, Onawole AT, Faye O, Shuaib DT. Understanding the corrosion inhibition of mild steel by selected green compounds using chemical quantum based assessments and molecular dynamics simulations. *J Mol Liq.* 2019;279:342–50.
 89. Innocenti M, Giaccherini A, Chelli R, Martinuzzi S, Giurlani W, Passaponti M, et al. Modelling of the Elementary Steps Involved in the Aluminum

- Electrochemical Deposition from Ionic Liquid Based Solution: The BMImCl/AlCl₃ System. *J Electrochem Soc.* 2019;167(1):13525.
90. Sasikumar Y, Adekunle AS, Olasunkanmi LO, Bahadur I, Baskar R, Kabanda MM, et al. Experimental, quantum chemical and Monte Carlo simulation studies on the corrosion inhibition of some alkyl imidazolium ionic liquids containing tetrafluoroborate anion on mild steel in acidic medium. *J Mol Liq.* 2015;211:105–18.
 91. Murulana LC, Singh AK, Shukla SK, Kabanda MM, Ebenso EE. Experimental and quantum chemical studies of some bis (trifluoromethyl-sulfonyl) imide imidazolium-based ionic liquids as corrosion inhibitors for mild steel in hydrochloric acid solution. *Ind Eng Chem Res.* 2012;51(40):13282–99.
 92. Ibrahim MAM, Omar EMA. Synergistic effect of ninhydrin and iodide ions during electrodeposition of zinc at steel electrodes. *Surf Coatings Technol.* 2013;226:7–16.
 93. Anicai L, Sin I, Brincoveanu O, Costovici S, Cotarta A, Cojocar A, et al. Electrodeposition of lead selenide films from ionic liquids based on choline chloride. *Appl Surf Sci.* 2019;475:803–12.
 94. Ibrahim MAM. Black nickel electrodeposition from a modified Watts bath. *J Appl Electrochem.* 2006;36(3):295–301.
 95. Li W, Hao J, Liu W, Mu S. Electrodeposition of nano Ni–Co alloy with (220) preferred orientation from choline chloride-urea: Electrochemical behavior and nucleation mechanism. *J Alloys Compd.* 2021;853:157158.
 96. Li Y, Zhang X, Hu A, Li M. Morphological variation of electrodeposited nanostructured Ni-Co alloy electrodes and their property for hydrogen evolution reaction. *Int J Hydrogen Energy.* 2018;43(49):22012–20.
 97. Yang Y-Y, Deng B. Preparation of Ni-Co alloy foils by electrodeposition. *Adv Chem Eng Sci.* 2011;1(02):27–32.
 98. Li B, Zhang W, Li D. Synthesis and properties of a novel Ni–Co and Ni–Co/ZrO₂ composite coating by DC electrodeposition. *J Alloys Compd.* 2020;821:153258.
 99. Ibrahim MAM, Alamri SN. Synergistic effect between PECTF and iodide ion on nickel electrodeposition from a Watts bath. *J Appl Surf Finish.* 2007;2:332–6.
 100. Bahramian A, Eyraud M, Vacandio F, Knauth P. Improving the corrosion

- properties of amorphous Ni-P thin films using different additives. *Surf Coatings Technol.* 2018;345:40–52.
101. Oliveira RP, Bertagnolli DC, Ferreira EA, da Silva L, Paula AS. Influence of Fe²⁺ oxidation and its antioxidant ascorbic acid as additive in Zn-Ni-Fe electrodeposition process on a low carbon steel. *Surf Coatings Technol.* 2018;349:874–84.
 102. Wu W, Eliaz N, Gileadi E. Electrodeposition of Re-Ni alloys from aqueous solutions with organic additives. *Thin Solid Films.* 2016;616:828–37.
 103. Yamauchi S, Nimura N, Kinoshita T. [Stabilization of ascorbic acid aqueous solution by protamine]. *Yakugaku Zasshi.* 1993 May;113(5):385–90.
 104. Hwang BJ, Santhanam R, Lin YL. Nucleation and growth mechanism of electroformation of polypyrrole on a heat-treated gold/highly oriented pyrolytic graphite. *Electrochim Acta.* 2001;46(18):2843–53.
 105. Asseli R, Benaicha M, Derbal S, Allam M, Dilmi O. Electrochemical nucleation and growth of Zn-Ni alloys from chloride citrate-based electrolyte. *J Electroanal Chem.* 2019;847:113261.
 106. Mardani R, Shahmirzaee H, Ershadifar H, Vahdani MR. Electrodeposition of Ni₃₂Fe₄₈Mo₂₀ and Ni₅₂Fe₃₃W₁₅ alloy film on Cu microwire from ionic liquid containing plating bath. *Surf Coatings Technol.* 2017;324:281–7.
 107. Caporali S, Marcantelli P, Chiappe C, Pomelli CS. Electrodeposition of transition metals from highly concentrated solutions of ionic liquids. *Surf Coatings Technol.* 2015;264:23–31.
 108. Barbato G. Electrodeposition of tantalum and niobium using ionic liquid. MSc.Thesis. University of Toronto; 2009.
 109. Endres F, Borisenko N, Al Salman R, Al Zoubi M, Prowald A, Carstens T, et al. Electrodeposition from ionic liquids: interface processes, ion effects, and macroporous structures. *Ion Liq Uncoiled Crit Expert Overviews.* 2012;1–27.
 110. Zhang QB, Hua YX, Wang YT, Lu HJ, Zhang XY. Effects of ionic liquid additive [BMIM] HSO₄ on copper electro-deposition from acidic sulfate electrolyte. *Hydrometallurgy.* 2009;98(3–4):291–7.
 111. Ong SP, Andreussi O, Wu Y, Marzari N, Ceder G. Electrochemical windows of room-temperature ionic liquids from molecular dynamics and density functional theory calculations. *Chem Mater.* 2011;23(11):2979–86.
 112. Hayyan M, Mjalli FS, Hashim MA, AlNashef IM, Mei TX. Investigating the

- electrochemical windows of ionic liquids. *J Ind Eng Chem*. 2013;19(1):106–12.
113. Omar IMA, Aziz M, Emran KM. Part I: Ni-Co Alloy Foils Electrodeposited Using Ionic Liquids. *Arab J Chem*. 2020;13:7707–19.
114. Lin M, Chen H, Dai H. Ionic Liquids Based Electrolytes for Rechargeable Batteries. *Mater Matters*. 2018;13:1.
115. Costovici S, Manea A-C, Visan T, Anicai L. Investigation of Ni-Mo and Co-Mo alloys electrodeposition involving choline chloride based ionic liquids. *Electrochim Acta*. 2016;207:97–111.
116. Raj MA, Arumainathan S. Comparative study of hydrogen evolution behavior of Nickel Cobalt and Nickel Cobalt Magnesium alloy film prepared by pulsed electrodeposition. *Vacuum*. 2019;160:461–6.
117. Varanasi JL, Veerubhotla R, Pandit S, Das D. Biohydrogen production using microbial electrolysis cell: recent advances and future prospects. *Microb Electrochem Technol*. 2019;843–69.
118. Prakash V, Sun ZHI, Sietsma J, Yang Y. Electrochemical recovery of rare earth elements from magnet scraps-a theoretical analysis. In: *ERES2014: 1st European Rare Earth Resources Conference| Milos*. 2014. p. 4–7.
119. Yuan J, Antonietti M. Poly (ionic liquid) s: Polymers expanding classical property profiles. *Polymer (Guildf)*. 2011;52(7):1469–82.
120. Foo KY, Hameed BH. Insights into the modeling of adsorption isotherm systems. *Chem Eng J*. 2010;156(1):2–10.
121. Emran KM, Al-Ahmadi AO, Torjoman BA, Ahmed NM, Sheekh SN. Corrosion and corrosion inhibition of cast Iron in hydrochloric acid (HCl) solution by cantaloupe (*Cucumis melo*) as green inhibitor. *African J Pure Appl Chem*. 2015;9(3):39–49.
122. Gholami M, Danaee I, Maddahy MH, RashvandAvei M. Correlated ab initio and electroanalytical study on inhibition behavior of 2-mercaptobenzothiazole and its thiole–thione tautomerism effect for the corrosion of steel (API 5L X52) in sulphuric acid solution. *Ind Eng Chem Res*. 2013;52(42):14875–89.
123. Ren X, Song Y, Liu A, Zhang J, Yuan G, Yang P, et al. Computational chemistry and electrochemical studies of adsorption behavior of organic additives during gold deposition in cyanide-free electrolytes. *Electrochim Acta*. 2015;176:10–7.
124. Omar IMA, Emran KM, Aziz M, Al-Fakih AM. A novel viewpoint of an

- imidazole derivative ionic liquid as an additive for cobalt and nickel electrodeposition. *RSC Adv.* 2020;10(53):32113–26.
125. Frisch M.J., Trucks G.W., Schlegel HB, Scuseria G.E., Robb M.A., Cheeseman J.R., Scalmani G., Barone V., Mennucci B., Petersson G.A., Nakatsuji H., Caricato M., Li X., Hratchian H.P., Izmaylov A.F., Bloino J., Zheng G., Sonnenberg J.L., Hada M., Ehara M., FDJ. gaussian09. Inc, Wallingford CT. 2009;121:150–66.
 126. El Adnani Z, Mcharfi M, Sfaira M, Benzakour M, Benjelloun AT, Hammouti B, et al. Reactivity and Fe complexation analysis of a series of quinoxaline derivatives used as steel corrosion inhibitors. *Struct Chem.* 2020;31(2):631–45.
 127. Belghiti ME, Bouazama S, Echihi S, Mahsoun A, Elmelouky A, Dafali A, et al. Understanding the adsorption of newly Benzylidene-aniline derivatives as a corrosion inhibitor for carbon steel in hydrochloric acid solution: Experimental, DFT and molecular dynamic simulation studies. *Arab J Chem.* 2020;13(1):1499–519.
 128. Rahmani H, Alaoui KI, Emran KM, El Hallaoui A, Taleb M, El Hajji S, et al. Experimental and DFT Investigation on the Corrosion Inhibition of Mild Steel by 1, 2, 3-Triazolereg Ioisomers in 1M Hydrochloric Acid Solution. 2018;
 129. Bouoidina A, El-Hajjaji F, Emran K, Belghiti ME, Elmelouky A, Taleb M, et al. Towards Understanding the Anticorrosive Mechanism of Novel Surfactant Based on Mentha pulegium Oil as Eco-friendly Bio-source of Mild Steel in Acid Medium. *Chem Res Chinese Univ.* 2019;35(1):85–100.
 130. Lallemand F, Comte D, Ricq L, Renaux P, Pagetti J, Dieppedale C, et al. Effects of organic additives on electroplated soft magnetic CoFeCr films. *Appl Surf Sci.* 2004;225(1–4):59–71.
 131. Huang FF, Huang ML. Complexation Behavior and Co-Electrodeposition Mechanism of Au-Sn Alloy in Highly Stable Non-Cyanide Bath. *J Electrochem Soc.* 2018;165(3):D152–9.
 132. Saha S, Sultana S, Islam MM, Rahman MM, Mollah MYA, Susan MABH. Electrodeposition of cobalt with tunable morphology from reverse micellar solution. *Ionics (Kiel).* 2014;20(8):1175–81.
 133. Ibrahim MA, Bakdash RS. New cyanide-free ammonia bath for brass alloy coatings on steel substrate by electrodeposition. *Int J Electrochem Sci.* 2015;10:9666–77.

134. Copeland TR, Skogerboe RK. Anodic stripping voltammetry. *Anal Chem.* 1974;46(14):1257A-1268a.
135. Pereira NM, Brincoveanu O, Pantazi AG, Pereira CM, Araujo JP, Silva AF, et al. Electrodeposition of Co and Co composites with carbon nanotubes using choline chloride-based ionic liquids. *Surf Coatings Technol.* 2017;324:451–62.
136. Feng Z, Li D, Sun Q, Wang L, Xing P, An M. Insight into the role and mechanism of 2, 2-bipyridine as a novel additive for nano-electrodeposition of Zn-Ni alloy. *J Alloys Compd.* 2018;765:1026–34.
137. Rahal H, Kihal R, Affoune AM, Rahal S. Electrodeposition and characterization of Cu₂O thin films using sodium thiosulfate as an additive for photovoltaic solar cells. *Chinese J Chem Eng.* 2018;26(2):421–7.
138. Al-Harbi AK, Emran KM. Effect of immersion time on electrochemical and morphology of new Fe-Co metal-metal glassy alloys in acid rain. *Arab J Chem.* 2019;12(1):134–41.
139. Emran KM, AL-Refai H. Electrochemical and surface investigation of Ni-Cr glassy alloys in nitric acid solution. *Int J Electrochem Sci.* 2017;12:6404–16.
140. Bakkar A, Neubert V. Electrodeposition of photovoltaic thin films from ionic liquids in ambient atmosphere: Gallium from a chloroaluminate ionic liquid. *J Electroanal Chem.* 2020;856:1–7.
141. Sun Y, Wang Z, Wang Y, Liu M, Li S, Tang L, et al. Improved transport of gold (I) from aurocyanide solution using a green ionic liquid-based polymer inclusion membrane with in-situ electrodeposition. *Chem Eng Res Des.* 2020;153:136–45.
142. Feng Z, Wang L, Li D, Sun Q, Lu P, Xing P, et al. Electrodeposition of Ni-Se in a chloride electrolyte: An insight of diffusion and nucleation mechanisms. *J Electroanal Chem.* 2019;847:1–8.
143. Emran KM, Ali SM, Alanazi HE. Novel hydrazine sensors based on Pd electrodeposited on highly dispersed lanthanide-doped TiO₂ nanotubes. *J Electroanal Chem.* 2020;856:113661.
144. Ibrahim MAM, Ismail EH, Bakdash RS. Copper-rich copper–zinc alloy coatings prepared by electrodeposition from glutamate complex electrolyte: current efficiency, Tafel kinetics and throwing power. *Trans IMF.* 2019;97(5):237–46.
145. Oliveira RP, Bertagnolli DC, Da Silva L, Ferreira EA, Paula AS, Da Fonseca

- GS. Effect of Fe and Co co-deposited separately with Zn-Ni by electrodeposition on ASTM A624 steel. *Appl Surf Sci.* 2017;420:53–62.
146. Sivasakthi P, Sangaranarayanan M V. Influence of pulse and direct current on electrodeposition of NiGd₂O₃ nanocomposite for micro hardness, wear resistance and corrosion resistance applications. *Compos Commun.* 2019;13:134–42.
 147. Lokhande AC, Bagi JS. Studies on enhancement of surface mechanical properties of electrodeposited Ni–Co alloy coatings due to saccharin additive. *Surf Coatings Technol.* 2014;258:225–31.
 148. Franklin TC. Some mechanisms of action of additives in electrodeposition processes. *Surf Coatings Technol.* 1987;30(4):415–28.
 149. Budi S, Kurniawan B, Mott DM, Maenosono S, Umar AA, Manaf A. Comparative trial of saccharin-added electrolyte for improving the structure of an electrodeposited magnetic FeCoNi thin film. *Thin Solid Films.* 2017;642:51–7.
 150. Chai Z, Jiang C. Electrochemical/chemical growth of porous (Ni, Co, Cu)(OH)₂ as an electrode material: Ternary Ni-Co-Cu nanocrystalline films corroded in neutral salt spray. *Electrochim Acta.* 2019;294:11–21.
 151. Liu P, Chen D, Wang Q, Xu P, Long M, Duan H. Crystal structure and mechanical properties of nickel–cobalt alloys with different compositions: A first-principles study. *J Phys Chem Solids.* 2020;137:109194.
 152. Gupta KP. The Co-Ni-Sn (Cobalt-Nickel-Tin) System. *J phase equilibria Diffus.* 2009;30(6):646–50.
 153. Pissolati NC, Majuste D. Morphology, roughness and microhardness of nickel electrodeposits produced in sulfate media on 316 L SS or Ti cathodes. *Hydrometallurgy.* 2018;175:193–202.
 154. Jiang QS, Cheng W, Li W, Yang Z, Zhang Y, Ji R, et al. One-step electrodeposition of amorphous nickel cobalt sulfides on FTO for high-efficiency dye-sensitized solar cells. *Mater Res Bull.* 2019;114:10–7.
 155. Shivakumara S, Naik YA, Achary G, Sachin HP, Venkatesha T V. Influence of condensation product on electrodeposition of Zn-Mn alloy on steel. *IJCT.* 2008;15:29–35.
 156. Shatla AS, Bawol PP, Baltruschat H. Adsorption of Iodide and Bromide on Au (111) Electrodes from Aprotic Electrolytes: Role of the Solvent.

- ChemElectroChem. 2020;7(23):4782–93.
157. Grignard V. Alkyl Halides & Aryl Halides. Synthesis (Stuttg). 1900;130:1322.
 158. Zohdy KM, El-Shamy AM, Kalmouch A, Gad EAM. The corrosion inhibition of (2Z, 2' Z)-4, 4'-(1, 2-phenylene bis (azanediyl)) bis (4-oxobut-2-enoic acid) for carbon steel in acidic media using DFT. Egypt J Pet. 2019;28(4):355–9.
 159. Singh P, Quraishi MA, Gupta SL, Dandia A. Investigation of the corrosion inhibition effect of 3-methyl-6-oxo-4-(thiophen-2-yl)-4, 5, 6, 7-tetrahydro-2H-pyrazolo [3, 4-b] pyridine-5-carbonitrile (TPP) on mild steel in hydrochloric acid. J Taibah Univ Sci. 2016;10(1):139–47.

APPENDIX F

LIST OF PUBLICATIONS

1. Omar, I.M.A., Emran, K.M., Aziz, M., and Al-Fakih, A.M. A novel viewpoint of an imidazole derivative ionic liquid as an additive for cobalt and nickel electrodeposition. *Royal Society of Chemistry Advance*. (2020). 10, 32113-32126. RSC Adv Impact Factor: 3.119. Journal Ranking in *Royal Society of Chemistry Advance*: Q2.
2. Omar, I.M.A., Emran, K.M., and Aziz, M. Part I: Ni-Co alloy foils electrodeposited using ionic liquids. *Arabian Journal of Chemistry* (2020) 13, 7707–7719. *Arabian Journal of Chemistry* Impact Factor: 4.762. Journal Ranking in *Arabian Journal of Chemistry*: Q2.
3. Omar, I.M.A., Emran, K.M., Aziz, M., and Al-Fakih, A.M. Part II: Impact of Ionic Liquids as Anticorrosives and Additives on Ni-Co Alloy Electrodeposition: Experimental and DFT study. *Arabian Journal of Chemistry* (2021) 14(1), 102909 . Impact Factor: 4.762. Journal Ranking in *Arabian Journal of Chemistry*: Q2. Accepted.
4. Omar, I.M.A., Emran, K.M., and Aziz, M. Electrodeposition of Ni-Co Film: A Review. *International Journal of Electrochemical Science* 16 (2021) 150962, doi: 10.20964/2021.01.16. Impact factor: 1.573. Journal Ranking in *Int. J. Electrochem. Sci*: Q4.
5. Omar, I.M.A., Emran, K.M., and Aziz, M. Impact of Ionic Liquid [FPIM]Br on the Electrodeposition of Ni and Co from an Aqueous Sulfate Bath. *Journal of Materials Research and Technology* (2021) 12,170-185. Impact factor: 5.289. Journal Ranking in *Journal of Materials Research and Technology*: Q1.